A proposal for a project at the CERN Antiproton Decelerator after LS2

Spectroscopic and gravitational measurements on antihydrogen: ALPHA-3, ALPHA-g and beyond

The ALPHA Collaboration
October 1st, 2019

Introduction: ALPHA so far

The ALPHA experiment was approved in 2005 and began operation at the AD in 2006. Our goal has always been to conduct the most precise possible tests of CPT symmetry by applying the techniques of modern atomic physics and metrology to antihydrogen. Given our deep theoretical and experimental understanding of the hydrogen atom, and its historical importance in the development of quantum theory, antihydrogen is an extremely compelling testbed of the foundations of modern physics. The original ALPHA apparatus was designed to demonstrate trapping of antihydrogen atoms; it did not initially have the capability to study their structure. The collaboration succeeded in trapping antihydrogen[1] in 2010, and all of our progress since then has built upon this seminal result. The approval of the ELENA ring by CERN management was closely linked to ALPHA's success with trapping at that time. We were shortly able to quickly demonstrate that we could store antihydrogen atoms long enough – initially up to 1000 s - to study their structure[2]. The interaction of electromagnetic radiation with antimatter atoms was observed in 2011, when we retrofitted the apparatus to allow the injection of microwave radiation. In the first-ever measurement of the structure of atomic antimatter[3], we were able to drive resonant interactions between the hyperfine quantum states of the anti-atoms. The original ALPHA machine was decommissioned in 2012, but not before we succeeded in demonstrating a method for making gravitational studies on trapped antimatter[4] and in exploring the charge neutrality of antihydrogen[5].

The ALPHA-2 apparatus (Figure 1) was constructed and installed in 2012, so that it could be commissioned before LS1 began in 2013. ALPHA-2 was designed to allow laser and microwave radiation to interact with trapped antihydrogen atoms. ALPHA-2 started in earnest in 2014, and the first publication in *Nature* appeared in 2016, when we greatly improved the charge neutrality measurement using a novel experimental technique[6]. Through years of development with ALPHA-2, we have managed to greatly improve the trapping efficiency for antihydrogen atoms. In the 2010 demonstration, we trapped, on average, one atom every eight trials, where a trial involves mixing antiproton and positron plasmas in the ALPHA-2 ion trap. Trials at that time could be repeated every twenty minutes or so. Today, we can trap 30 atoms of antihydrogen per trial, and a trial requires about four minutes. We have also developed techniques for accumulating, or 'stacking' antihydrogen atoms[7], and can now routinely accumulate and store more than 1000 atoms, collected over several hours of AD beamtime.

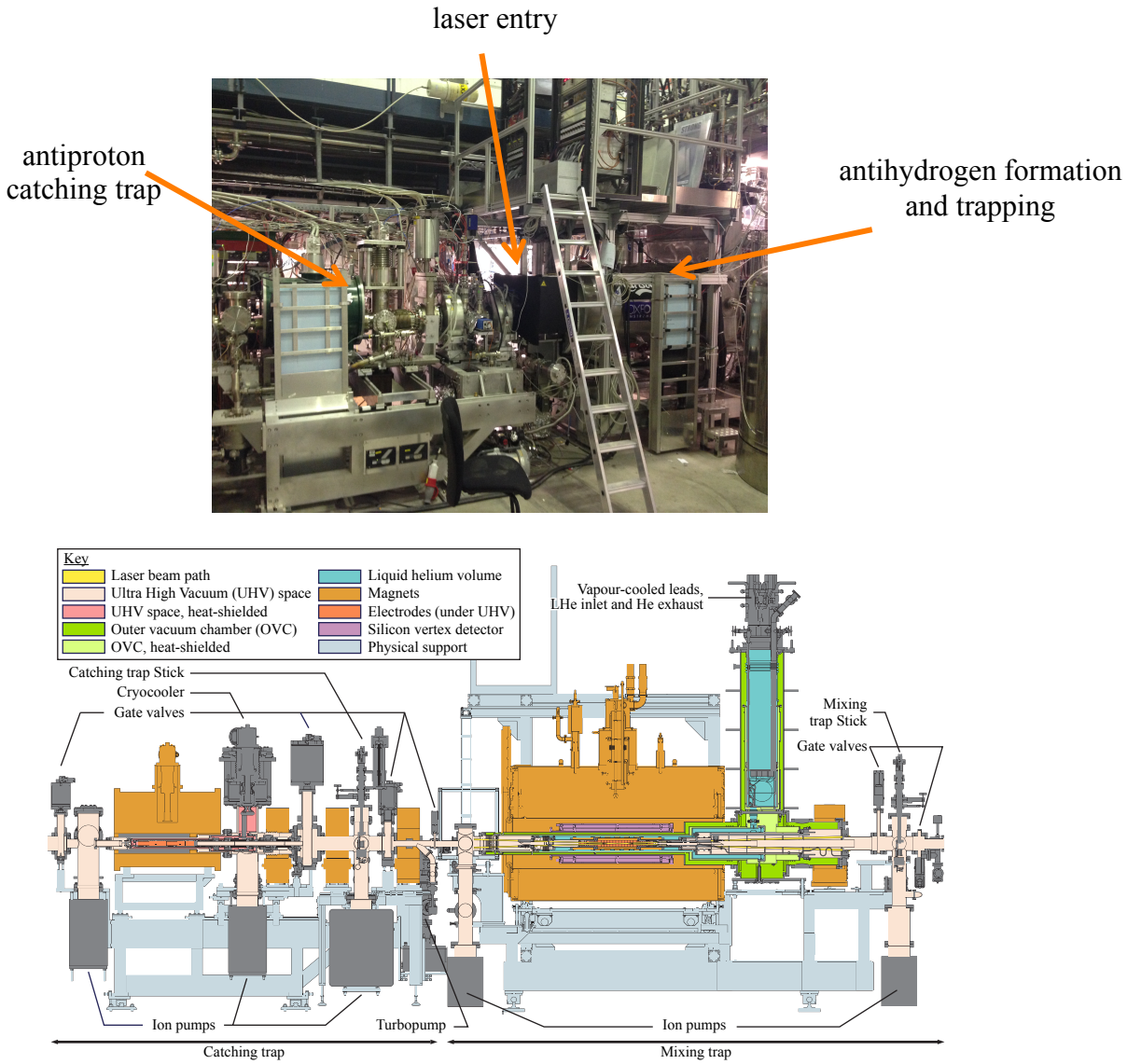

Figure 1. Views of the ALPHA-2 apparatus. Antiprotons from the AD enter from the left and are captured in the catching trap. They are mixed with positrons to form antihydrogen in the main apparatus, which houses Penning traps for confining charged particles, the magnetic trap for confining antihydrogen, and the silicon vertex detector for antiproton annihilations. The positron accumulator is to the right of the main apparatus and not pictured here.

In parallel, we have developed laser sources for antihydrogen spectroscopy in ALPHA-2. The first physics breakthrough came during the 2016 run, when we observed the 1S-2S transition in trapped antihydrogen[8]. This transition has long been the 'Holy Grail' of low energy antimatter studies and was one of the main justifications for constructing the AD back in the late 1990's. The equivalent transition frequency in hydrogen is known[9] with an absolute precision of order 10^{-15}. Our latest measurement in antihydrogen[10], published in 2018, has a relative uncertainty of about 10^{-12}. One of the main goals of the ALPHA physics program after LS2 is to work towards hydrogen-like precision for

this transition, in order to provide the most sensitive possible experimental test of CPT symmetry using antimatter. See Section 1, below.

We have also continued to make progress on the hyperfine studies with antihydrogen. The first detailed characterization of the spectrum of the hyperfine transitions was published[11] in *Nature* in 2017. The latest work on this type of physics is currently under review at *Nature*[12] and will be described in Section 2 below.

The third prong in the ALPHA physics program with antihydrogen involves the Lyman-alpha, or 1S-2P, transition. ALPHA has developed a unique, pulsed laser source[13] for the 121 nm (vacuum ultraviolet) light to probe these levels. The first observation of the Lyman-alpha transition in antihydrogen was reported in *Nature* in 2018[14]. This represents the first measurement on a state having orbital angular momentum, and the new capabilities have lead to rapid advancements in other aspects of our physics program, to be described below.

The year 2018 was the last year of AD operations before LS2. ALPHA undertook a very ambitious plan both to continue the experimental spectroscopy program and to install and commission the ALPHA-g apparatus for gravitational studies. ALPHA requested and the SPSC approved, an unprecedented redistribution of our beamtime, featuring an eight-week pause in the middle of the Run to allow for ALPHA-g installation. This strategy was very successful, as ALPHA-g was installed and operated with antiprotons and positrons, and we achieved important new physics results with ALPHA-2. The first of these results, a detailed study of the antihydrogen fine structure and a determination of the Lamb shift[15], is currently under review at *Nature.* See Section4 below.

The pulsed, Lyman-alpha laser was also used to demonstrate the first laser cooling of antimatter during the 2018 run. We believe this to be a revolutionary change in anti-atomic physics. We have already seen a dramatic effect of laser cooling on the experimental linewidth of the 1S-2S transition in antihydrogen. Each of these advances is the subject of an article that is in preparation; both will be submitted in the near future with the goal of simultaneous publication in *Nature*. The details are discussed in Sections 1 and 4 below. Laser cooling of antihydrogen will also be employed in the new ALPHA-g experiment, with profound implications for the obtainable precision of gravity measurements. See section 5.

We are currently undertaking a major upgrade to our capabilities for all types of spectroscopy. This effort is collectively referred to as ALPHA-3 and is described in sections 1 to 4 below. In the following, we use the name 'spectroscopy trap' to refer to the modified apparatus and to distinguish it from antihydrogen traps in ALPHA-g.

The ALPHA-g experiment (Figure 2) will use ALPHA's demonstrated trapping and detection developments to study antimatter gravitation. ALPHA-g was recommended for approval by the SPSC in October of 2016. ALPHA-g essentially comprises a vertically oriented trap for antihydrogen and a large time projection chamber (TPC) detector for locating the annihilation positions of anti-atoms that are released from the trap. The initial goal of the experiment is to determine the sign of the gravitational acceleration on antimatter. Future experiments will determine the magnitude of the acceleration with precision of 1% or better. The ALPHA-g apparatus, including the new beamline to connect it to ALPHA-2 and the positron accumulator, was installed between May and

November of 2018. ALPHA-g was operational for a few weeks before the shutdown for LS2. We were able to transfer and trap antiprotons and positrons, to commission the TPC and measure antiproton annihilation distributions, but the run ended before we could synthesize antihydrogen. The future physics program with ALPHA-g is described in Section 5.

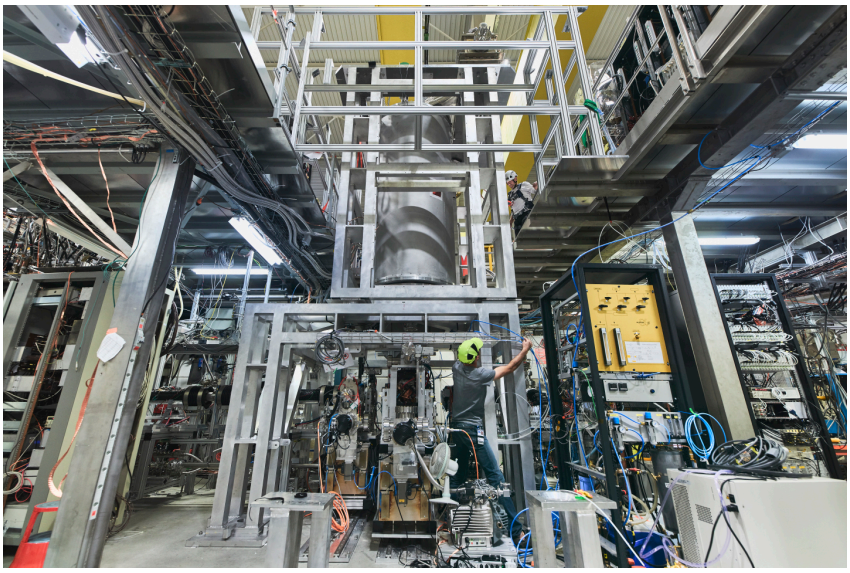

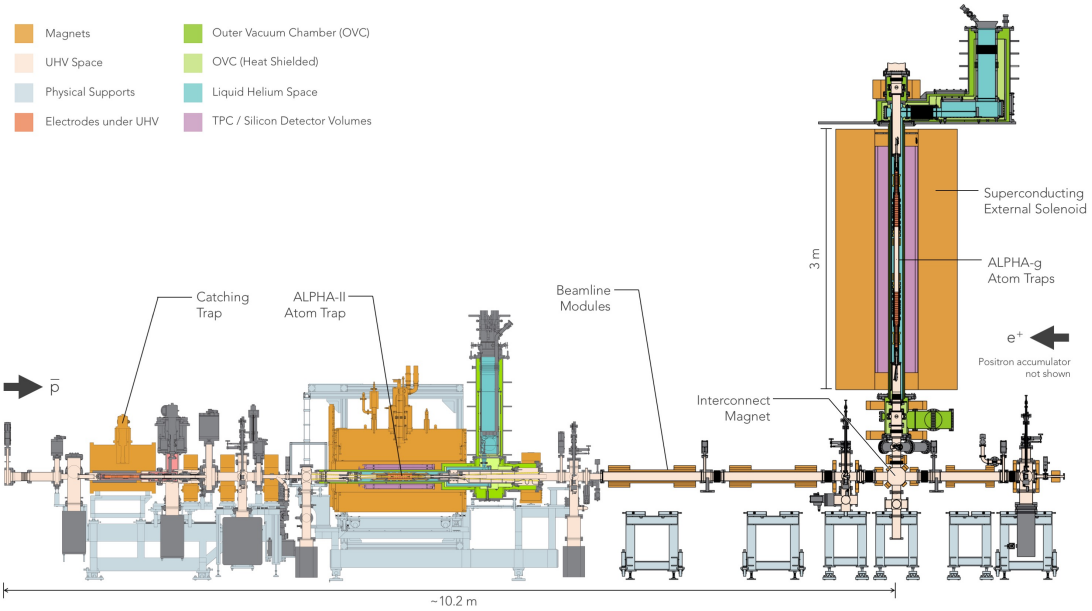

Figure 2. The ALPHA-2 and ALPHA-g configuration. The positron accumulator (not illustrated) is to the right of the diagram.

Below, we describe in detail the state of antihydrogen physics in ALPHA and our ambitious vision for future experiments that will fully utilize the capabilities of the AD/ELENA complex for the foreseeable future.

Section 1. Spectroscopy of the 1S-2S transition in antihydrogen

State of the art

Spectroscopy of the 1S-2S transition in antihydrogen has been envisioned since before the first antihydrogen was formed at LEAR in 1995[16] (see R. Neumann[17]and H. Herr[18] for early discussions). It is the most precisely measured transition in hydrogen[19], and it is therefore a very attractive transition to study antihydrogen and hydrogen as a way of testing symmetry in nature. However, apart from creating antihydrogen, a number of hurdles had to be overcome to achieve a first measurement in antihydrogen. The low number of antihydrogen atoms available meant that the most compelling route to spectroscopy involved trapping of the anti-atoms to allow for long interrogation times to compensate for the low numbers. ALPHA successfully trapped antihydrogen for the first time in 2010[1], however, initially only about one atom was trapped every 2 hours. The fundamental challenge here is that even the deepest traps for confining ground-state (anti)hydrogen through interaction with its dipole moment only allow trapping of atoms with kinetic energies below ~50 μeV, or ~0.5 K in temperature units. This can be compared to the initial energies of the trapped antiprotons, which are up to a few keV after they are slowed and captured from the AD. The current apparatus is shown schematically in Figure 3. We will not revisit the details of antihydrogen production and trapping here, as these are covered in many references[8,10,11].

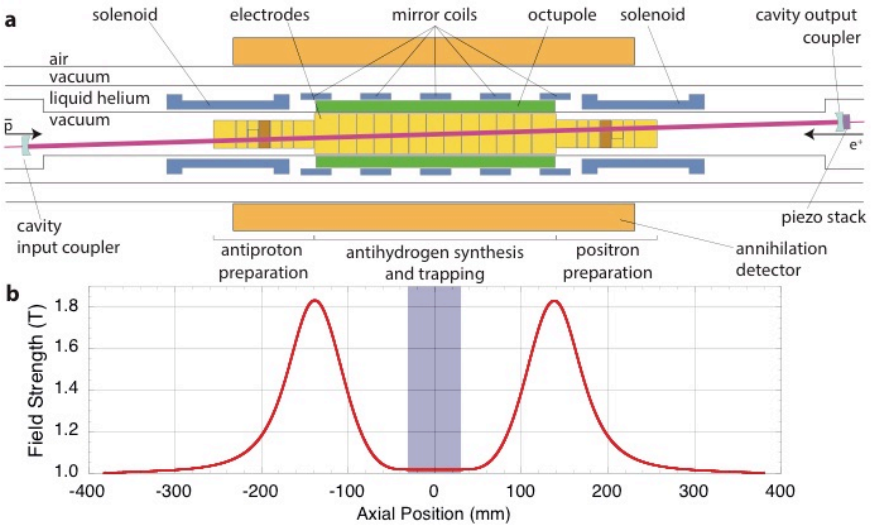

Figure 3. The ALPHA-2 central apparatus and magnetic field profile. a. The various Penning traps (electrodes + 1 T external solenoid, not shown) confine and manipulate antiprotons and positrons to produce antihydrogen. Cold (< 0.5 K) anti-atoms are confined radially by the octupole field and axially by the magnetic well formed by the five mirror coils and plotted in b. Earlier experiments in ALPHA used only the end mirror coils. The flattened profile here (uniform to ± 10^{-4} T on axis in the shaded region) extends the laser resonance volume and slightly improves the depth of the neutral atom trap. Laser light enters from the

antiproton side (left in the figure) and is aligned with the fixed axis of the optical enhancement cavity. The laser beam crosses the trap axis at an angle of 2.3°. The piezoelectric actuator on the output coupler is used to lock the cavity to the laser frequency. The two figures have the same axial scale; the radial extent of the annihilation detector is larger than illustrated. The central region of the apparatus is cooled by the liquid helium bath for the superconducting trapping magnets.

We have improved the trapping performance drastically[7] since 2010. Today, Mixing about 100,000 antiprotons with 3 million positrons leads to up to 30 antihydrogen atoms trapped in a single trial, requiring about 4 minutes. The other major hurdle to antimatter spectroscopy was available laser power. The 1S

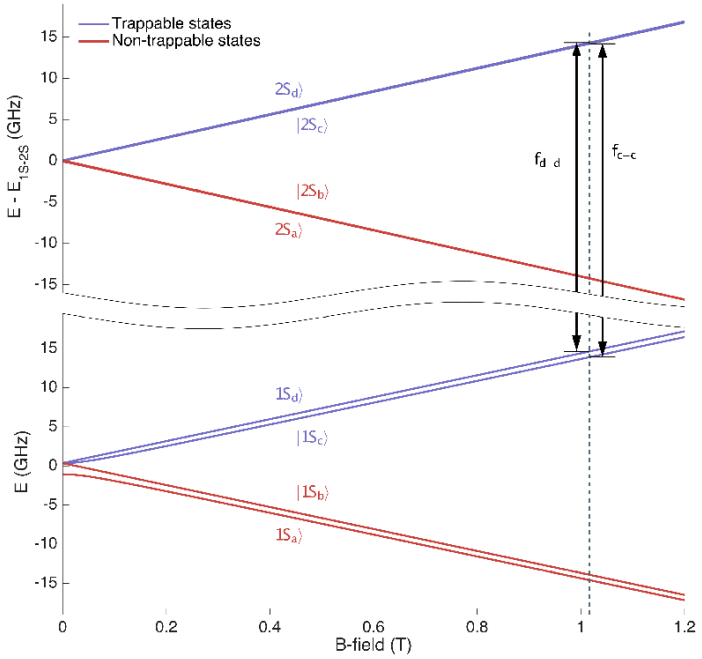

Figure 4. Energy levels in the 1S and 2S states of hydrogen as a function of magnetic field strength. The dashed line indicates the field at the minimum of the ALPHA antihydrogen trap. The two transitions we can study are labeled d-d and c-c.

to 2S transition (see Figure 4) is a two-photon transition, which is advantageous as it means that (a) the first order Doppler shift is eliminated through use of counter-propagating photons and (b) once on resonance the laser will interact with all the atoms independent of their velocity class. However, the interaction probability is low, so, with the relatively few atoms available, the first excitation of the *1S-2S* transition in antihydrogen required a cryogenic, optical resonant cavity (Figure 3) to build up about 1 W of the 243 nm light needed for the excitation. After some initial trials in 2015, this feat was first accomplished at the end of the 2016 run, and in total about 650 anti-atoms (in 33 trials) were used for the first observation, and the trapped anti-atoms were exposed to the laser for 10 minutes in each trial[8]. Resonant interaction can be observed if the atoms are excited to the *2S* state by two photons. The excited atoms can then be ionized by a third photon, in which case they are lost from the trap. The excited atoms might also decay to an untrappable state (Figure 4) in which case they are

also lost. The first observation[8] involved a simple on-resonant and off-resonant comparison of the fate of the trapped atoms. It took five days to collect the data.

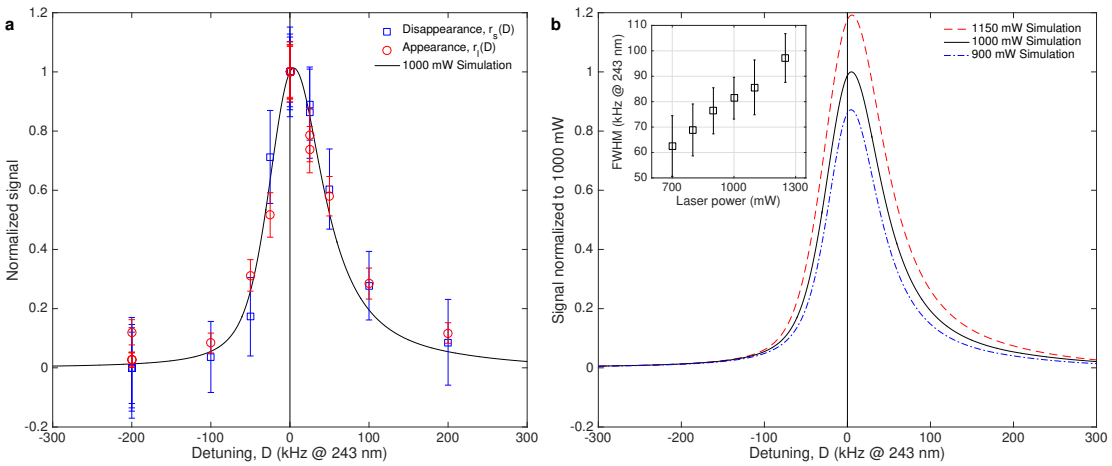

Figure 5. Antihydrogen spectral lines. a. The simulated curve (not a fit, drawn for qualitative comparison only) is for 1000 mW stored cavity power and is scaled to the data at zero detuning. For the experimental points, 'Appearance' refers to annihilations that are detected during laser irradiation; 'Disappearance' refers to atoms apparently missing from the surviving sample. b. Three simulated lineshapes (for hydrogen) are depicted for different cavity powers to illustrate the effect of power on the size and the frequency at the peak. The width of the simulated line as a function of power is plotted in the inset.

In 2017 we were able to trap atoms much more effectively by using special techniques to reduce the e^+ temperature and by accumulating antihydrogen using our novel accumulation technique[7]. This increase allowed the first measurement of the *1S-2S* line-shape[10] (reproduced in Figure 5) and determination of the transition frequency to a precision of 2×10^{-12}. This measurement was done with about 16,000 antihydrogen atoms. For operational reasons, dominated by the negative effects on antihydrogen formation of illuminating the experimental chamber with 243 nm light, measuring this line shape took 10 weeks of real time. As presented to the SPSC in January 2019, we recently cleared the last operational hurdles and started accumulating antihydrogen for almost the full eight hours of a typical AD shift. This has caused a paradigm shift in how we can operate, in that it has allowed us to accumulate close to 2000 atoms in the trap. With such numbers we can measure a *1S-2S* line shape in a single run by scanning the laser across the resonance and detecting the annihilations induced. With about 1 W of laser light in the trap we were able to reproduce the 2017 line-shape measurement in a single day in 2018 - to be contrasted to the original 10 weeks. Figure 6 shows the results of two such measurements on consecutive days of the 2018 AD Run. As will be discussed in Section 4 below, we had, by then, implemented laser-cooling on the 1S-2P transition for the *d* hyperfine states (*d* referring to the antiproton spin being anti-parallel to the local magnetic field). The effect of laser cooling is evidenced by the narrow line width of the cooled sample, whereas the un-cooled c-states exhibit a much larger linewidth. (Although the linewidth is Doppler-free to first order, the line is transit-time broadened because the atoms traverse the laser beam as they orbit in the trap. Cooling their motion reduces this contribution in a manner consistent with our simulations of the process.) These measurements took ~19 hours of real time, starting with about 11 hours of antihydrogen accumulation, followed by an additional six hours of laser-cooling, until we

finally could sweep the 243 nm laser frequency across the transition (~100 times to reduce the influence of depletion of anti-atoms) in about 2h. We thus kept antihydrogen atoms trapped for almost a full day in these experiments.

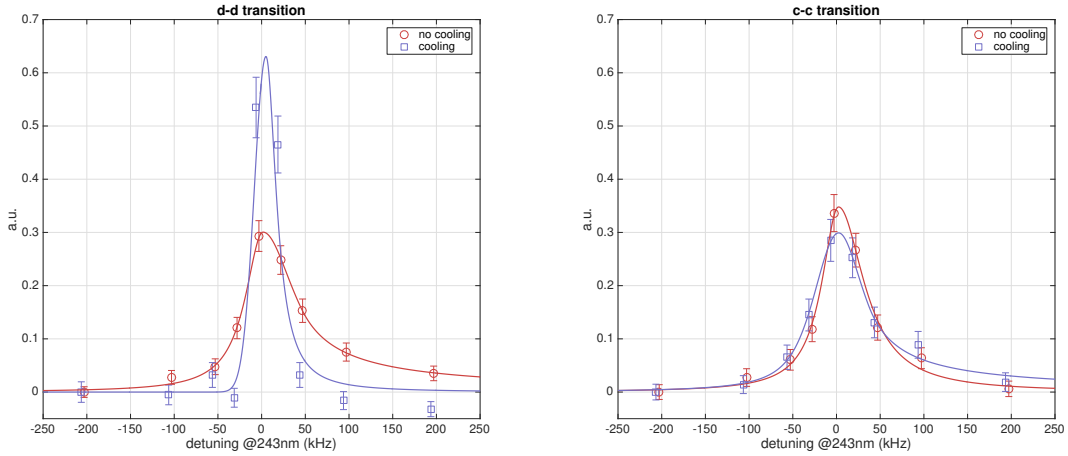

Figure 6. Preliminary line shapes of the 1S-2S two photon transitions in antihydrogen recorded from a trapped sample of antihydrogen with more than 900 atoms in each. Laser cooling was applied to the d-state atoms in the blue samples. Each curve took less than a day of real time to record. **ALPHA Preliminary**

Laser spectroscopy in a magnetic trap naturally suffers from potential systematic issues stemming from the frequency shifts induced by the large magnetic fields. To be able to control these systematics we have progressively improved our ability to measure magnetic fields using electron-cyclotron-resonance (ECR). Our initial method relied on observing the electron plasma modes and their response to microwave heating around the cyclotron resonance, and achieved a resolution of around 0.3 mT at the trap center in the inhomogeneous trapping fields[20]. Recent developments that consist of using repeated electron plasma temperature measurements have improved the resolution to ~0.01 mT. The *1S* and *2S* magnetic field-induced level shifts are slightly different, and in the region around 1 T this difference results in frequency shifts of 962 Hz/mT and 18.6 kHz/mT for the *d-d* and *c-c* lines respectively[21]. This difference motivated the choice of the *d-d* line for the first line-shape measurement, where our state-of-the-art magnetic field diagnostic made magnetic field uncertainties negligible with respect to determining the uncertainty on the line center frequency. However, the asymmetry in the line shapes in Figure 5 and Figure 6 is largely due to the presence of the trap magnetic fields, and these fields could thus affect the precision with which the line center can be determined. We have therefore investigated and confirmed that we can de-energise the main solenoid magnet of the Spectroscopy Trap *after* antihydrogen accumulation while still retaining about 80% of the trapped atoms. In combination with laser-cooling (see Section 4), we should be able to additionally reduce the main trapping fields without further losses, and thus conduct spectroscopic measurements in lower magnetic fields in an effort to both investigate and minimize the influence of the magnetic systematic effects.

Planned improvements to the apparatus during LS2

With thousands of anti-atoms available for experimentation, a number that will likely increase [see Sections 6 and 7], a range of new possibilities is opened. The ability to do a spectrum in a single day allows for exploration of the systematic effects that influence the measurement, as well as of course such issues as potential sidereal or other variations caused by, for example, an inhomogeneous distribution of dark matter[22], fifth-forces[23] or Lorentz invariance violation[24]. An additional possibility with a sample of this size is the direct observation of light emitted from the anti-atoms. Until now, all of our measurements have been destructive, in that the measurements were based on the dependence on an annihilation signal of antihydrogen in resonance with the radiation. This stems from the near unity efficiency with which we can detect such annihilations, relative to the rather less effective alternatives – due to solid angle and quantum efficiency limitations - for fluorescent photon detection. With thousands of atoms simultaneously trapped, it is suddenly no longer prohibitively difficult to observe the photons from the decays of the anti-atoms. The advantages are obvious: (a) The experiment can be done many times over with the same sample (b) there will be no depletion effects and (c) the same method can be used to do experiments with hydrogen, thus eliminating some issues of interpretation. We are thus planning the integration of photon-detectors in our cryogenic trap system during LS2 in order to monitor photons emitted from trapped antihydrogen.

The goal of all our efforts in *1S-2S* spectroscopy is to approach, and perhaps to surpass the precision of the hydrogen *1S-2S* measurements to achieve the most precise and accurate matter-antimatter comparison that is possible. The line widths of laser-cooled antihydrogen shown in Figure 6 are narrower than the uncooled one, and simulations[25] show that a temperature of 20 mK is possible with our current hardware, in which case the line width becomes a few kHz, comparable to the line width in current state-of-the-art hydrogen spectroscopy[19].

In order to support improved resolution and accuracy on the 1S-2S transition we therefore plan, under the ALPHA-3 project, the following interventions on our Spectroscopy Trap:

(a) Addition of photon detection inside the cryogenic environment, adjacent to the trapping region.
(b) Modification of the optical enhancement cavity to effect a doubling of the size of the beam-waist. This should halve the transit-time broadening and thus result in improved resolution.
(c) Introduction of laser-cooled Be^+ ions to sympathetically cool positrons, in order to increase the trapping efficiency (see Section 7) and thereby the statistics of our measurements.

In addition we will upgrade the laser-systems and the metrology components of our setup. Our frequency measurements currently rely on a combination of commercial Cs clocks borrowed from CERN and a GPS disciplined quartz

oscillator. The absolute precision of these systems is just below 10^{-12} on our experimental timescale. Our laser-system is stabilized by a commercial ULE (ultra low expansion) cavity to a linewidth of ~1 Hz, which is sufficient for the foreseeable future. In order to achieve the same precision as in hydrogen we are thus focusing on implementing better absolute frequency references. We are targeting three somewhat complementary/redundant improvements to the absolute frequency information needed for our goals:

(a) We will acquire and install an active hydrogen maser and reference it to UTC(OP) from SYRTE in Paris via a GPS Common View setup[26]. This should result in an absolute frequency reference at a level of 10^{-14} in less than a day, and 10^{-15} in less than a week. This system has been ordered and will be ready for operation when beam returns in 2021.

(b) We will purchase and install a Cs-fountain clock[27]. This will give us an independent absolute frequency reference of 10^{-15} in less than a day. This is not an off-the-shelf commercial product and is a physics experiment in itself. With a delivery of about 18 months we expect it to be operational and implemented in our frequency chain for the 2022 run.

(c) We are in discussions with both METAS (the Swiss national metrology institute) in Bern and SYRTE (the French equivalent) in Paris about what it takes to be connected to their respectively planned and existing fiber networks for frequency comparisons. These networks will allow us to compare our Cs-Fountain with the world standard of clocks at the 10^{-15} level at least. This would be a strong complement to the comparisons we can do with GPS Common View and add crucial redundancy to the setup. Setting this up will require some CERN services to be involved. We have no timescale for this at the moment.

Maximum performance of the active maser and the Cs-Fountain requires them to be installed in an electromagnetically quiet location. They therefore cannot be installed in our current laser laboratory, which is adjacent to the AD. Neither can they be installed too far from our laser laboratory. A new, quiet, air-conditioned room is therefore needed in building 393. The improvements described here and later in this proposal, and related to antihydrogen spectroscopy, comprise the ALPHA-3 upgrade program. ALPHA-3 will re-use the existing atom trap and external solenoid magnets and the silicon vertex detector, but will feature a new insert for the Penning traps and the laser pathways. The internal upgrades must be ready at the end of LS2.

As discussed in Section 4, we will also consolidate the Lyman-alpha laser-system to allow laser-cooling to be applied at will to any spectroscopic or other antihydrogen measurements we are doing. Finally, for completeness we have also started activities aiming at making cold, trappable hydrogen that can be trapped in our antihydrogen trap. Ultimately, doing the same measurement on hydrogen and antihydrogen alternately in the same environment will be extremely compelling.

Physics goals and milestones

Our goal is to measure the energy of the *1S-2S* transition in antihydrogen such that we approach and eventually surpass the current accuracy and precision in hydrogen. In order to achieve this goal we have laid out the initial physics milestones for the 2021 and 2022 runs below.

1) Achieve 10^{-13} absolute frequency accuracy on our experimental time scale.
2) Measure the 1S-2S transition energy at 1T to a precision of 10^{-13} or better using laser-cooled antihydrogen.
3) Measure the 1S-2S transition energy at or below 0.05T to a precision of 10^{-13} or better using laser-cooled antihydrogen.

It should, however, be noted already here that the commissioning and the initial measurement program of ALPHA-g will be our first physics priority after LS2.

Section 2. Microwave measurements: ground-state hyperfine intervals and the Lamb shift

The zero-field hyperfine splitting frequency a/h of hydrogen is one of the most important atomic intervals ever studied. At one point in time it was the most precisely measured quantity in physics. It is known to 13 significant figures, with an absolute precision of about 1 mHz. The measurement of hyperfine intervals in free or magnetically-trapped antihydrogen, leading to direct spectroscopic comparisons with analogous intervals in hydrogen, has long been viewed as a compelling strategy for conducting precision experimental tests of fundamental symmetries and potential physics beyond the Standard Model. Of particular interest to ALPHA is the magnetic dipole transition between the two trappable states, *c* and *d*. The frequency of this interval passes through a maximum in a magnetic field of about 0.65 Tesla, which is advantageous for spectroscopy; see Figure 7. Moreover, within the context of the Standard Model Extension (SME), this interval is nominally sensitive to Lorentz and CPT-violating effects. (Irrespective theoretical frameworks such as the SME, which identify particular intervals as good candidates for probing physics beyond the standard model, our philosophy has been to pursue any and all opportunities to characterize the properties of the antihydrogen atom.)

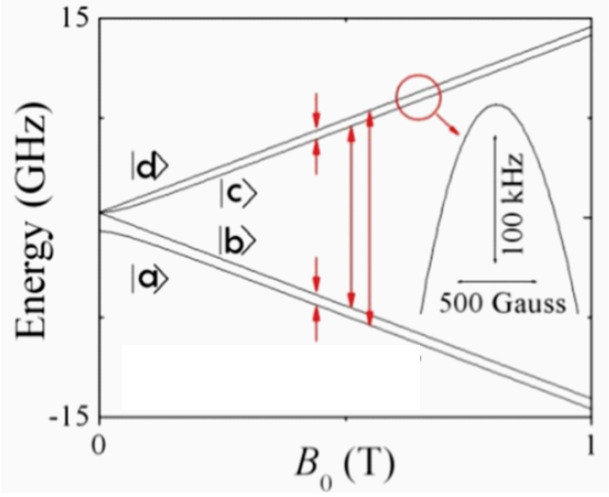

Figure 7 Breit-Rabi diagram for the ground electronic (positronic) state of the hydrogen (antihydrogen) atom. Arrows indicate transitions that can be induced when an oscillating magnetic field $\boldsymbol{B}_1$ is applied perpendicular to the static magnetic field $\boldsymbol{B}_0$. To date, hyperfine spectroscopy experiments performed by ALPHA have focused on the *c* to *b* and *d* to *a* positron spin resonance (PSR) transitions in magnetic fields of order 1 Tesla. Future experiments will focus on the *d* to *c* NMR (nuclear magnetic resonance) transition. Inset: The frequency of the d to c transition in the vicinity of the maximum, which occurs in a 0.65 Tesla magnetic field.

State of the Art

We have performed three experiments that characterize the 1420 MHz ground state hyperfine splitting of antihydrogen, at increasing levels of precision. All three involve measurements of the frequencies at which the *d* to *a* and the *c* to *b* transitions occur; see **Figure 7**.

To the extent these positron spin flip (or positron spin resonance: PSR) transitions occur in the same magnetic field, the difference between the two frequencies that are measured is nominally equal to the hyperfine splitting. The first experiment[3], reported in 2012, marked the advent of antimatter spectroscopy and set a rudimentary bound of 100 MHz on a/h. The second experiment[11], reported in 2017, revealed a spectral distribution characteristic of the two transitions, and constrained a/h to an absolute precision 0.5 MHz. The third experiment, described in a manuscript[12] that is presently under review at Nature, yields a/h to an absolute precision of 13 kHz, or a relative precision of 9 parts-per-million (ppm), and is consistent with expectations for hydrogen. This accomplishment represents the state of the art, insofar as measurements of hyperfine intervals in antihydrogen are concerned.

The experiment is performed in largely the same flattened trap field configuration used in our optical spectroscopy experiments (**Figure 3**), except for the fact that we intentionally generate a shallow absolute minimum at the centre of the trap. The depth of this depression, with respect to other local minima in the 1 T base field, is of order 0.5 Gauss. The existence, location, and profile of the absolute minimum are independently verified with electron cyclotron resonance (ECR) experiments that map the distribution of fields along the trap axis.

For this experiment, atoms are trapped and then subjected to microwave radiation that is injected (Figure 8) at monotonically increasing frequencies, in the

form of a staircase function. First, the frequency is swept over the onset of the lower (*c* to *b*) PSR line at about 28 GHz to identify the minimum frequency at which atoms come into resonance. Irradiation continues until all *c*-state atoms are ejected from the trap. The frequency is then raised by 1.42 GHz and the procedure is repeated to identify the onset of the *d* to *a* transition. Nominally, the hyperfine splitting is equal to the difference between the microwave irradiation frequencies during the two time bins identified as onsets. In detail, however, magnetic field drift effects complicate this simple interpretation of data. The data and the techniques used for dealing with magnetic field drifts will not be reproduced here, as the manuscript is still under consideration.

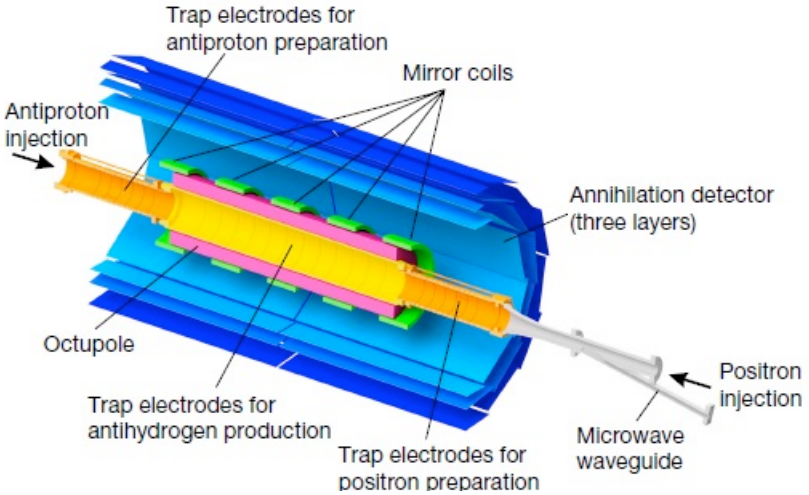

Figure 8. Cut-away schematic of the ALPHA-2 antihydrogen production and trapping region, illustrating the injection of microwaves via the waveguide at the right of the figure.

Planned improvements to the apparatus during LS2

The key technical innovation we will incorporate to advance precision measurements of hyperfine intervals is an electromagnetic resonator capable of sustaining an ultra-high frequency (UHF) oscillating magnetic field directed perpendicular to the trap axis. This will enable us to drive transitions between trapped *c* and *d*-state atoms, and ultimately to measure the frequency of that interval as a function of magnetic field; see Figure 7. Note that direct irradiation of antihydrogen down the trap axis, as is done in our PSR spectroscopy experiments (**Figure 8**) is not possible. This is because the Penning trap electrode stack acts as a waveguide below cutoff at the relevant frequencies.

The design constraints on the UHF resonator are severe. It must produce a transverse $\boldsymbol{B}_1$ field (to induce the appropriate transition), it must be positioned at the axial minimum in $\mathbf{B}_0$ (to make the transition spectroscopically relevant), it must possess a high degree of cylindrical symmetry (so the dynamics of charged particles on axis are not perturbed by their images), it must be very thin (so that the depth of the magnetic potential well confining antihydrogen is not compromised), and it ought to be squat (since the axial dimension sets the resolution of the electrostatic trap). Beyond this, its tuning must be correct at cryogenic temperatures and it must be mechanically robust.

We have constructed a number of prototype resonators that meet the criteria listed above, and which yield suitably intense $\boldsymbol{B}_1$ fields at reasonable power levels. We are investigating how to incorporate such a resonator in the upgraded insert of the ALPHA-3 project.

Physics goals and milestones

Our goal is to measure the c-d transition frequency at the turning point $B^* = 0.65$ Tesla (cf. inset to Figure 7), which is directly linked to the zero-field hyperfine splitting frequency a/h. That is, $f_{cd}^* = (a/h)\left[1/2 - \sqrt{\eta}/(1+\eta)\right]$ where $\eta = \gamma_{\bar{p}}/\gamma_{e^+}$ is the ratio of the antiproton and positron gyromagnetic ratios; hence $f_{cd}^* = 655$ MHz. Operating at this turning point suppresses sensitivity to magnetic field variations, and thus directly addresses the limiting factor in measurements of ground state hyperfine intervals we have performed to date. It simultaneously maximizes atom-field interaction times, and hence maximizes attainable frequency resolution. Note that a complementary minimum exists in the *a*-*b* transition at precisely the same magnetic field; the only experimental investigations of this turning point of which we are aware were performed by our recently-retired ALPHA colleague, W. Hardy.

The procedure for detecting transitions between the low-field seeking *c* and *d* states involves three spin-state manipulations. First, the *b*-*c* PSR transition is irradiated to clear the trap of *c*-state atoms. Second, the *c*-*d* NMR transition is irradiated to transfer *d*-state atoms to the *c*-state. Finally, the *b*-*c* PSR transition is re-irradiated while monitoring the Si-vertex detector to identify spin-flip induced annihilation events.

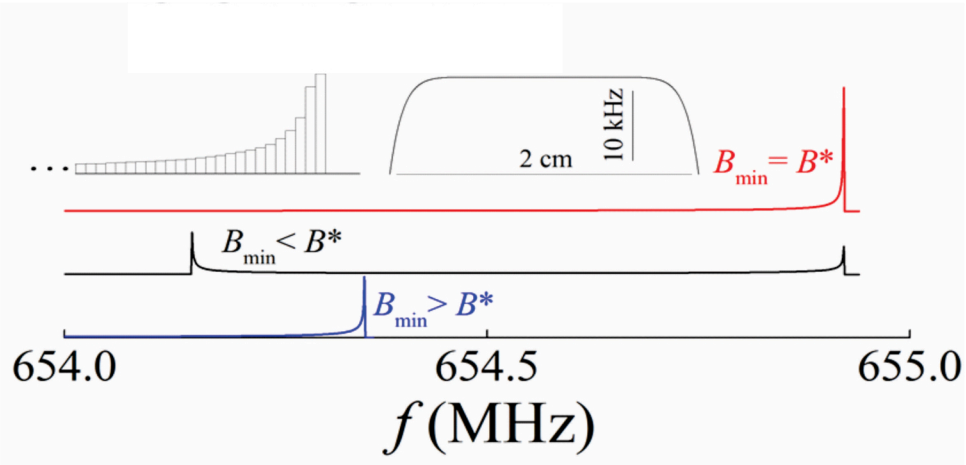

Figure 9. Calculated distribution of c-d (or NMR) transition frequencies for a trap field configuration similar to that employed in our early measurements of the ground state hyperfine splitting[3,11]. Top left: relative intensities near the maximum at $f_{cd}^* = 655$ MHz (10 kHz bins). Top right: variation of f_{cd}^* across the trap diameter. The spectroscopic feature associated with B_{min} is much more abrupt than pictured here, when a flattened field configuration is employed.

Figure 9 shows a schematic depiction of the distribution of NMR frequencies anticipated for low-field seeking atoms under three conditions:

$B_{min} < B^*$, $B_{min} = B^*$, and $B_{min} > B^*$, where B_{min} is the minimum field in the trap. With $B_{min} > B^*$, a sharp rise in intensity occurs on the high-frequency side of the distribution; this is associated with atoms passing through the minimum field at the centre of the trap. With $B_{min} < B^*$ two sharp features are evident: the high- and low-frequency features are associated with transitions as atoms transit surfaces over which $B = B^*$ and as they pass through the minimum field in the trap, respectively. When $B_{min} = B^*$ these two features coalesce; the turning point in the transition frequency occurs at the turning point in field and the resulting spectroscopic feature is maximally intense. In particular, the key feature of this distribution in which we are interested – its extreme upper edge at f_{cd}^* – becomes maximally abrupt (inset to Figure 9). Also shown in Figure 9 is the variation of the transition frequency f_{cd} as a function of radial position, near the centre of the trap with $B_{min} = B^*$.

We anticipate a staged approach to measurements of f_{cd}^* that will enable us to evaluate and address any unforeseen systematic effects. In this context a reasonable target for a first demonstration-level experiment is to probe f_{cd}^* to the level where transit-time broadening effects (finite coherent atom-field interaction times) begin to play a role. In round numbers this would yield a sub-kHz frequency measurement, or perhaps several hundred parts-per-billion (ppb) relative to the zero-field hyperfine splitting a/h. Next we envision transitioning to the use of laser-cooled antihydrogen, which in turn will permit significant reductions in trap depth. The combined effect of these factors will be to increase atom-field interaction times by an order of magnitude, thereby enabling a measurement of f_{cd}^* to several tens of ppb relative to a/h. At this stage, further progress would require a concerted effort to perform systematic studies, to acquire statistics, and to understand and characterize the detailed form of spectroscopic features in the data. Here it seems reasonable to anticipate that one might gain a factor 10 in precision through what would effectively amount to "line splitting." Altogether, we anticipate that a measurement of f_{cd}^* at the level of a few Hz, or a few parts per billion relative to a/h is plausible on a five year timescale. On absolute frequency or energy scale, this is competitive with our proposal for the precision to which the *1S* to *2S* interval will eventually be measured. Increases in precision beyond this level will require new innovations.

Microwave measurements of the Lamb shift

The measurement of the hydrogen Lamb shift[28] was one of the most important events in modern physics and helped trigger the development of quantum electrodynamics. In recent years, the hydrogen Lamb shift has gained renewed interest because it is sensitive to the charge radius of the proton, and improved Lamb shift measurements may help to resolve the ongoing proton size puzzle[29 30,31,32]. The antihydrogen Lamb shift is therefore of considerable fundamental interest. ALPHA has recently succeeded in determining the Lamb shift in antihydrogen via optical excitations of the *1S – 2S* and *1S – 2P* transitions[15], as a by-product of laser cooling efforts. However, this result was the combination of measurements from separate experiments and the precision was limited by the Doppler broadening of the *1S – 2P* line. Alternatively, it should also be possible to directly excite the *2S – 2P* transition in trapped antihydrogen with

resonant microwave radiation. Microwave methods have the advantage that the Doppler broadening is almost negligible. In addition, the microwave system should give a much higher signal rate and is much lower maintenance than the 121 nm laser system.

Starting with a sample of trapped antihydrogen in the *1S* ground state, we can introduce CW or pulsed 243 nm laser-light to excite the two-photon *1S – 2S* transition. Simultaneously, we inject microwave radiation with a swept frequency near the $2S_a$ to $2P_f$ transition (Figure 10). Antihydrogen atoms that are driven into the $2P_f$ state will quickly decay to the 1S state and the majority (~85%) will end up in an untrapped state and annihilate on the trap walls[21] The $2S_a$ to $2P_f$ transition frequency can then be measured at a number of different magnetic fields such that we can extrapolate to obtain the zero-field Lamb shift. At 1 T the $2S_a$ to $2P_f$ transition can be excited by microwaves at roughly 24 GHz. This is within the range of the current ALPHA-2 and ALPHA-g microwave hardware.

There will be several experimental challenges including distinguishing signal from background annihilations due to laser ionized antihydrogen and background mixing to the *2P* state from the motional electric field that atoms experience in the magnetic trap. Detailed simulations are needed to determine optimal experimental parameters (laser power, microwave power, microwave sweep rate, etc.), expected lineshape, and achievable precision. In addition, detailed characterization of the microwave mode structure over a range of frequencies will be required. Changing the magnetic field will influence the behaviour of antimatter plasmas and of the resonant microwave mode structure. Detailed studies of these effects as a function of magnetic field will also be critical for ECR magnetometry and for NMR spectroscopy at 0.65 T (see above). In the longer term, increased precision could be obtained by working at much lower magnetic fields (<0.2 T) or in a field-free region. At these low fields, the resonant microwave frequencies are below the cutoff frequency of the Penning trap, and internal UHF resonators, as described above, will be required.

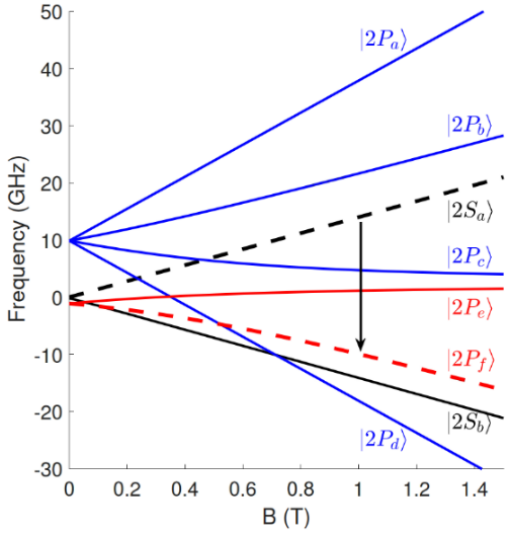

Figure 10. n=2 energy levels as a function of magnetic field strength. The antiproton spin has been neglected here.

Section 3. Other laser spectroscopic measurements on antihydrogen

Physics motivation

In hydrogen, the fine structure arising from the Dirac Equation only depends on the total angular momentum of the electron. For example, the $2S_{1/2}$ and $2P_{1/2}$ states have exactly the same energy despite differing by one unit of orbital angular momentum. In 1947 Lamb and Retherford discovered a difference of about 1 GHz between the levels in the real hydrogen atom[28]. The eponymous Lamb-shift is a consequence of the electron interacting with itself, vacuum polarization and the finite probability of the electron being inside the nucleus.

The Lamb-shift in hydrogen can be determined directly by coupling levels in the n=2 manifold by microwave radiation. The most precise result yields the $2S_{1/2}$ Lamb-shift with a precision of 3 ppm[32]. By determining the frequency interval of two (or more) lines it is possible to extract the Rydberg constant, R_∞, and the rms-charge radius of the proton, r_p, which contributes about 10^{-4} to the total Lamb-shift, from a linear combination. The Lamb-shift scales with n^{-3}, and therefore the ground-state Lamb-shift is $\sim$8 GHz with a $\sim$1 MHz contribution from the nucleus. Since the *1S-2S* transition is already determined with a high accuracy in antihydrogen, laser spectroscopy of transitions to energy levels with principal quantum number n>2 is a compelling route to precisely determining properties of the nucleus.

While Lamb's result was foundational for the development of Quantum Electrodynamics, measurements of r_p have recently sparked a controversy known as the proton radius puzzle. In 2010, a laser spectroscopic measurement of the Lamb-shift in muonic hydrogen yielded a value of r_p which is 5σ smaller than the result from electron-proton scattering data[33]. A subsequent measurement[34] widened the gap to 7σ. Recent measurements in (electronic) hydrogen on the *2S-4P* line also result in a smaller value[35], while the result from spectroscopy on the *1S-3S* is in line with the larger value from scattering data[36]. Determining r_p from the most recent direct electronic Lamb-shift measurement yields a value[37] consistent with muonic hydrogen. While this agreement suggests that muons do not differ from electrons in the way they interact with protons, discrepancies between measurements remain unresolved.

Naturally, given our current capabilities to perform precision spectroscopy of trapped antihydrogen, we aim for a measurement of the antiproton charge radius, $r_{\bar{p}}$. The precision in two-photon laser spectroscopy in ALPHA has, since the first observation of the *1S-2S* transition, already been sensitive enough to resolve $r_{\bar{p}}$. In a landmark achievement, the Lamb-shift was determined from a combination of the *1S-2S* frequency and an observation of fine structure[15] (see Section 4) However, the Doppler shift leads to insufficient precision to isolate the contribution from the nucleus. Our goal is to measure the transition frequency of other lines with enough precision to allow a unique determination of $r_{\bar{p}}$ and $\bar{R}_\infty$ in antihydrogen. The measurement is of fundamental significance in determining properties of the antiproton. It also widens the scope of testing fundamental symmetry with antihydrogen by including the nucleus.

Planned improvements to the apparatus during LS2

Excited states with n=3 and n=4 have natural line widths of order 1 MHz for S-states and of order 10 MHz for P and D-states. In order to determine the transition frequency with enough resolution to resolve $r_{\bar{p}}$, two-photon spectroscopy will be used in the ALPHA-3 apparatus to remove the Doppler-shift to first order. The two-photon excitation geometry will be realised by using one of the existing laser-paths that intersect the centre of the magnetic trap. The central trapping apparatus will be modified to accommodate for the new wavelengths and for reducing laser scatter. Our laser suite will need to be complemented by additional solid-state lasers which will need to be referenced to our frequency metrology (See Section 1). Further modifications will be necessary to deliver the laser beams to the experiment. Here, we will employ fibre-optical photonics as much as is practicable.

Detection of antihydrogen in excited states with n>2 will rely on a resonant interaction which renders the anti-atom untrappable via spin-flips or ionisation, leading to a signal in the silicon vertex detector. In addition, the apparatus will be modified to enable collection and better internal detection of antiprotons lost due to resonant ionisation. As stated in Section 1, the internal trapping structure will also be modified to accommodate silicon photomultiplier arrays which can directly detect fluorescence photons.

Improved control of the background magnetic field will be necessary to allow for experiments at fields below 1 T at which the fine structure in excited states with n>2 yields the optimum excitation signal, and ultimately for measurements exploring a range of magnetic field magnitudes including low fields. Magnetometry methods will be developed to cover the extended range of fields.

Physics goals and milestones

Ultimately, we aim to achieve a precision that allows a comparison to the proton charge radius. This goal presents a formidable challenge due to complications in the energy level structure arising from the 1 T background field that the ALPHA magnetic trap is immersed in for manipulation of charged particles in the Penning traps. The main milestones will be:

I. Observation of a transition to an excited state with n>2. Simulations indicate that the excitation rate from the *2S* state to the *3S* and *3D* states is favourable in comparison with the roughly 50 ms lifetime of the trapped antihydrogen atom in the *2S* state. Since solid-state lasers with enough power are readily available commercially, this transition is a good candidate for initial experiments. However, we will not rule out experiments on the *1S-3S* and *2S-4(S,D)* transitions, and microwave transitions within the n=2 manifold. Experiments on optical transitions require development of lasers and build-up cavities while experiments within the n=2 manifold will need upgraded delivery of microwaves. The signal will be produced via resonant loss of antiatoms in the standard fashion requiring no new detector technology.

II. Observation of fluorescence from trapped antihydrogen. Fluorescence detection offers the tantalising prospect of observing light emitted from

antimatter atoms in the laboratory for the first time. While it is inconceivable that the central emission and absorption wavelengths of one line would not match, an observation of emission nevertheless holds intrinsic philosophical value. Scientifically this step holds great significance since fluorescence detection enables precision spectroscopic experiments without depleting the trapped antihydrogen sample, and thus rapid experiments with large samples of antihydrogen.

III. Characterisation of the signal to show statistical sensitivity to $r_{\bar{p}}$. Control of systematic effects and determination of $r_{\bar{p}}$ with an accuracy of 1%.

Section 4. Lyman-alpha spectroscopy and laser-cooling of antihydrogen

State of the art

Slowing of the translational motion of atoms by momentum impact of near resonant photons, known as laser cooling, has revolutionized atomic physics in the past decades. Application of such a technique to antimatter has long been a dream for researchers in our field. In 2018, we have been able to realize this dream in ALPHA.

The ultimate precision of *1S-2S* laser and hyperfine microwave spectroscopy in magnetic traps will be limited by the uniformity of the magnetic field probed by trapped anti-atoms (Zeeman broadening), as well as transit-time broadening (which is proportional to the atom's speed). A sample of extremely cold antihydrogen that only accesses a small portion of the trap will minimize these effects. Furthermore, laser cooling is an essential tool for precision measurement of gravitational forces on antihydrogen using the ALPHA-g apparatus (Section 5).

Doppler cooling of antihydrogen can take place via radiation pressure from Lyman-alpha (Ly-α) light at 121.6 nm, which drives the *1S-2P* transition. ALPHA members have proposed and performed detailed and realistic calculations for pulsed laser cooling in the ALPHA-2 geometry, where optical access is limited to one dimension[25]. Their numerical calculations showed that Doppler cooling of antihydrogen to ~20 mK can be achieved within a few hundred seconds using pulsed 121.6 nm radiation with a linewidth of 100 MHz and a pulse energy of 0.1 μJ at a 10 Hz repetition rate.

(a) Lyman-alpha laser development

Historically, generation of Ly-α radiation has been a challenging task, because of the lack of tunable lasers or non-linear crystals for these very short wavelengths, and the impossibility of transmitting this radiation through air (thus its classification as vacuum ultraviolet (VUV) radiation). A major technical achievement of ALPHA over the past few years has been the development of a narrow-line, solid-state based, pulsed Ly-α source using a third harmonic generation (THG) configuration in Kr/Ar mixed gas. At ALPHA, the vacuum ultraviolet radiation at 121.6 nm is produced in two steps: frequency doubling of 730-nm pulses followed by third harmonic generation in a high-pressure Kr/Ar gas cell. The schematic diagram of the laser system is shown in Figure 11 [38].

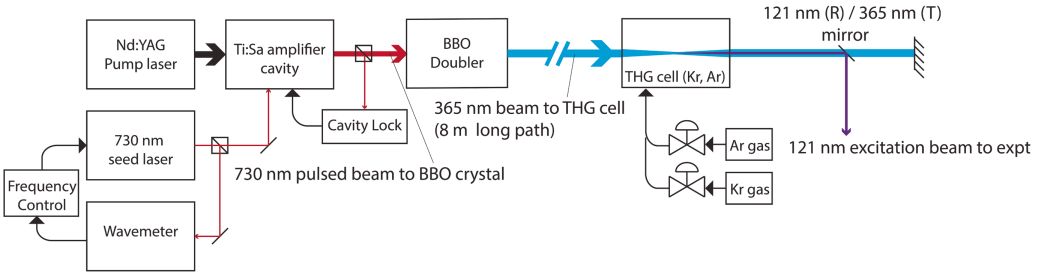

Figure 11. Ly-α Laser system at ALPHA. The figure shows a schematic of the 121.6-nm laser system for driving the 1S–2P transition.

730 nm pulses produced by pulse amplification of narrow linewidth (<100 kHz), continuous-wave radiation (TOPTICA diode laser) in two Ti:Sapphire crystals are converted to 365 nm by frequency doubling in a beta barium borate (BBO) crystal. The third harmonic of 365 nm is generated in a high-pressure Kr/Ar gas cell (total pressure about 4 bar) after focusing the 365-nm pulses (15 mJ - 20 mJ) with an ultraviolet-grade lens (focal length 150 mm). The generated 121.6 nm pulses have a pulse energy of up to 8 nJ right after the THG cell, corresponding to the conversion efficiency of 5×10^{-7}. (Some groups quote the values inside the cell: in this case we have a conversion efficiency of 10^{-6}, and an average power of 0.2 μW). The typical pulse width and linewidth at 121.6 nm are 12 ns and 65 MHz (FWHM, estimated). We have also developed an optical transportation and alignment system for 121.6 nm, a very significant effort given the technical challenges associated with the VUV light. We have obtained a high transport efficiency (~25%) into the UHV volume, resulting in a pulse energy of ~ 2 nJ inside the ALPHA-2 antihydrogen trap regions. This corresponds to an average power of ~20 nW, overlapping with trapped antihydrogen atoms.

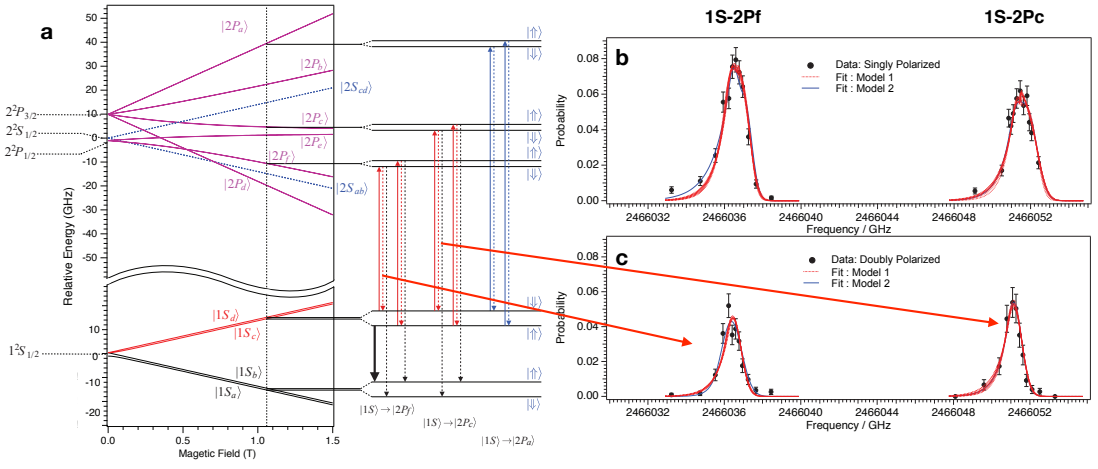

Figure 12. a. Energy levels of the *1S*, *2S* and *2P* states of hydrogen under magnetic fields. The vertical red arrows indicate the $1S_{cd}$-$2P_c$ and $1S_{cd}$-$2P_f$ one-photon transitions that are detected via the spin flipping to the untrappable levels (shown by the dashed black arrows). The vertical blue arrows indicate the cooling $1S_{cd}$-$2P_a$ transitions. b. Detected signals from the trappable $1S_c$ and $1S_d$ states to the $2P_f$ and $2P_c$ states. c. Detected signals after the depletion of the $1S_c$ states by the microwave transition of $1S_c$-$1S_b$ (shown as a black arrow).

Observation of the 1S-2P Lyman-alpha transition

After several years of intense development of the 121 nm Lyman-alpha laser system, we were able to observe the *1S-2P* Ly-α transition of magnetically trapped antihydrogen during the beam time in 2017. There are three fine structure levels in the *2P* state that are accessible from the magnetically trapped $1S_{cd}$ states. They are the $2P_a$, $2P_c$ and $2P_f$ states shown in **Figure 12**a.

When antihydrogen is excited to the $2P_c$ or $2P_f$ state, it decays to the ground state manifold within a few ns by emitting a photon at 121.6 nm. The mixed nature of the positron spin states in the $2P_c$ and $2P_f$ states implies that these states can decay to the $1S_b$ (or $1S_a$) states via a positron spin flip (black dashed arrows in **Figure 11**). Atoms in these final states are expelled from the trap, resulting in their annihilations on the trap walls. Annihilation products (mostly charged pions) are in turn detected by the silicon vertex detector. Because the laser is pulsed, and the excitation light is present for about 12 ns for each pulse, the annihilation events due to the excitation are only expected to occur in the approximately 1-ms time window in which the untrapped atoms are forced to the trap wall. This greatly helps us to distinguish between signals due to laser-driven annihilations and those due to cosmic background. As a result, we have successfully observed annihilation signals after excitations from the trappable $1S_c$ and $1S_d$ state to the $2P_c$ states (**Figure 12**b).

The observed transitions have a spectral linewidth of about 1.5 GHz (full-width at half-maximum, FWHM)., corresponding to the convolution of the Doppler width (~1 GHz at 350 mK) and the hyperfine splitting (0.7 GHz) between the ground $1S_c$ and $1S_d$ states at 1 T. A detailed analysis for the $2P_c$ transition has been published in *Nature*[14]. This represents the first observation of the *1S-2P* Lyman-alpha transition in anti-matter atoms. The corresponding transition in hydrogen is one of the most fundamental atomic processes in the Universe, and has relevance to cosmological phenomena such as cosmic recombination in the early Universe. This transition also forms the basis for laser cooling of antihydrogen.

Fine structure and the Lamb shift in antihydrogen

Subsequent to the initial observation of *1S-2P* transition, we have resolved, for the first time, the fine structure in antihydrogen[15]. In this measurement, doubly spin polarized antihydrogen has been prepared and probed with Lyman-alpha laser light. Double polarization has been achieved by depleting the $1S_c$ hyperfine state via inducing microwave transition between the trappable $1S_c$ state and the un-trapped $1S_b$ state, prior to the *1S-2P* excitation. As a result, a narrower linewidth has been obtained, as shown in **Figure 12**c.

The observed ~1 GHz FWHM of these lines is in agreement with the Doppler width expected for our trapping conditions. Detailed analysis showed the consistency, at the 1.6×10^{-8} level, between the obtained antihydrogen transition frequencies with those expected for hydrogen at 1 T, providing a new test of CPT invariance involving the orbital angular degree of freedom to 16 parts per billion.

Furthermore, we have been able to determine the Lamb shift in antihydrogen by combing these results with our earlier measurement of the *1S-2S* transition frequency. The observation of the Lamb shift in atomic hydrogen was a landmark discovery that led to development of renormalizable QED, arguably the most precise physical theory in existence to date. Here, we have been able to extract the corresponding quantity in antimatter system for the first time. Based on our measurements at 1 T, by assuming the standard Zeeman Hamiltonian, we determined the zero-field fine structure splitting to be 10.88 ± 0.19 GHz and the Lamb shift to be 0.99 ± 0.11 GHz for antihydrogen. The resulting values are consistent with the predictions of QED at the 2% and 11% level, respectively[15]. These observations represent an important step towards a precision measurement of the fine structure and the Lamb shift in the antihydrogen spectrum as tests of charge-parity-time (CPT) symmetry [39], and towards the determination of other fundamental quantities, such as the antiproton charge radius[40], in this antimatter system.

Demonstration of antihydrogen laser cooling

In the final days of the ALPHA-2 run in the summer of 2018, just before our effort was switched to ALPHA-g, we have been able to demonstrate the first-ever laser cooling of antihydrogen atoms. After several hours of continuous irradiation of 10 Hz, 121.6 nm pulses at the $1S_d$-$2P_a$ cooling transition (**Figure 12**) a significant narrowing of the linewidth of the $1S_d$-$2P_c$ transition was observed with the cooling laser slightly red detuned (***Figure 13***(a) blue lines) relative to the non-cooling width (***Figure 13***(a) green line), while a broadening of the linewidth was observed with the cooling laser slightly blue detuned to the (***Figure 13***(a) red line). The linewidth of the $1S_d$-$2P_c$ transition is affected by Doppler broadening, and therefore the narrowed spectral line indicates that the velocity of antihydrogen parallel to the cooling/probing laser beam was reduced by the cooling pulses. In addition, we have observed an increase in the time-of-flight of spin flipped antihydrogen between the excitation of the $1S_d$-$2P_c$ probing transition and the arrival at the wall for cooled atoms (***Figure 13***(b)). This indicates that the cooling of antihydrogen was also realized for the transverse (radial) direction, implying that three-dimensional cooling was realized with a single axis laser access. Furthermore, laser cooled antihydrogen samples were used in the *1S-2S* measurements, where we have observed a narrowing of the linewidth of this transition (see Section 1). Demonstration of laser cooling is another paradigm shift in antimatter studies with far reaching implications.

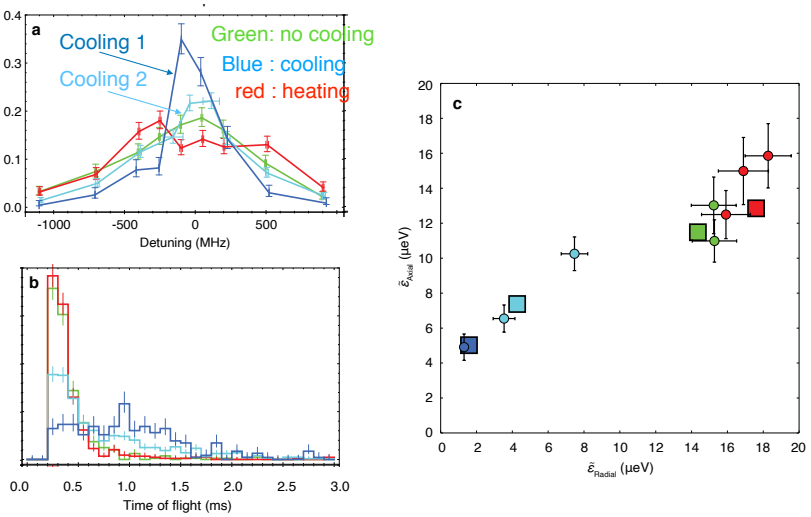

Figure 13. *Preliminary results of laser cooling. (a) The lineshapes of the 1Sd-*2Pc transition obtained with (green) no laser cooling, (light and dark blue) after cooling, and (red) after heating. Cooling 1 series had 4 hours of laser cooling applied, in Cooling 2 series laser cooling was applied during 5 hours of antihydrogen accumulation phase, followed by 6 hours of laser cooling phase. (b) The time-of-flight distribution of spin-flipped antihydrogen after the 1Sd-2Pc probe excitation. Colors are the same as in (a). (c) Deduced radial and axial energies of antihydrogen. filled circles: experimental data, filled squares: simulation.

Planned improvements to the apparatus during LS2

Improvement of the Lyman-alpha cooling laser: In order to improve the cooling efficiency and achieve the lowest possible temperatures, we will improve the existing laser system over the next few years. Key improvements will be (1) the increase of the repetition rate from 10 Hz to 50 Hz, (2) the increase of the 121.6 nm pulse energy, (3) the improvement of the pulse-to-pulse stability in both frequency and energy, and (4) the automation of all alignment systems. The increase of the repetition rate will be done by replacing the 532 nm Nd:YAG laser for the pump of the 730 nm Ti:Sapphire pulse amplifier. The spatial mode and pointing stability of our 50 Hz Nd:YAG laser is not as good as that of the 10 Hz Nd:YAG laser. Therefore we will install a spatial filter and a beam pointing stabilizer before the Ti:Sapphire pulse amplifier. The increase of the 121.6 nm pulse energy will be achieved by (a) increasing the 365 nm pulse energy by improving the spatial beam quality and adding another BBO crystal, and by (b) using an ultra-clean gas handling systems for the Kr/Ar gas mixture. The current SHG conversion effeiciency from 730 nm to 365 nm is still less that 20 %, which is mainly limited by the spatial beam quality. By installing a spatial filer and another BBO crystal, one should be able to achieve a 30 % conversion efficiency, yielding >30 mJ at 365 nm. Furthermore, we will replace the existing THG cell and its gas handling system by an ultra-clean system using electro-polished stainless steel materials, such that we can employ a tight focusing configuration for the 121.6 nm generation. This will increase the 121nm pulse energy at least five to ten times, which will reduce the cooling time significantly.

Currently the 121.6 nm power fluctuates over 20 %. A part of the reason is the inhomogeneity of the mixed gas in the THG cell due to the slow diffusion of gases in a high pressure cell. In order to improve the stability of the power, we

will install a static gas mixer before the THG cell. In addition, we will modify the laser cavity lock system to improve the pulse-to-pulse frequency stability. We will also install auto alignment systems for the 365 nm path and 121.6 nm path in order to improve a long term stability during laser cooling.

(b) Development of the ALPHA-g laser cooling system: For the laser cooling of antihydrogen in the ALPHA-g trap, we will develop an independent THG cell and a new optical transport system with an auto-aligner underneath the vertical ALPHA-g apparatus. Since the optical aperture of the ALPHA-g trap is wider than that of the ALPHA-II trap, we will expand the 121.6 nm laser beam to allow for an increased overlap with the trapped antihydrogen. Furthermore, we will install a folding mirror at the top of the ALPHA-g trap to retro-reflect the 121.6 nm cooling laser for more efficient cooling.

(c) Development of a narrow band Lyman-beta laser at 102.6 nm: With the success of the generation of narrow band Ly-α pulses and the *1S-2P* spectroscopy and laser cooling of antihydrogen, it is straightforward to develop a narrow band Lyman-beta (Ly-β) laser at 102.6 nm for the *1S-3P* excitation of antihydrogen. The development of the Ly-β laser radiation will also be useful for future ALPHA experiments requiring population of *2S* state antihydrogen (see, *e.g.* [41]). These include *2S-nS* and *2S-2P* Lamb shift experiments, as well as some future initiatives. For the demonstration of the generation of 102.6 nm and spectroscopy of *1S-3P* of (anti)hydrogen, we will use the THG scheme but in a jet of Ar gas using 307.8 nm pulses, which can be generated by THG of 923.4 nm generated by a similar Ti:Sapphire pulse amplification system and a linear cavity. For the STImulated Raman Adiabatic Passage (STIRAP) excitation to the 2S state via 3P state, we may need nano-second pulses with a pulse energy of up to 1 μJ. If necessary, we would increase the pulse energy at 102.6 nm by using a sum frequency four wave mixing (FWM) in Xe via the $5P^5 6p$ state (2×249.6 nm+575.6 nm). In order to deliver the VUV pulses at 102.6 nm into the trap chamber, we will construct a four-stage differential pumping systems between the VUV generation region and the trap chamber.

Physics goals and milestones

(a) Laser cooling of antihydrogen to the lowest possible temperatures

While our initial laser cooling demonstration stands as an important milestone, quantitative understanding of the cooling process will require intensive systematic studies and hardware improvements. Our short-term goals include introducing improvements leading to robust methods for routine laser cooling, as well as achieving temperatures below 20 mK, consistent with simulations of the current trap geometry.

Systematic studies of the cooling process:

We will undertake a campaign to quantitatively understand and optimize the cooling process. At present, some discrepancies exist between our simulations and data, insofar as the final energies attained are concerned. A key issue is the motion of the trapped antihydrogen in our magnetic trap. We attribute the fact we achieve three-dimensional cooling with a single axis laser to

a coupling of degrees of freedom. This coupling, which is possibly a bottleneck in the cooling rate, could be enhanced by increasing the non-harmonicity of the trapping potential. There is large parameter space to explore, including laser frequencies (detuning, sweeping) and variations in magnetic trapping potential (both static and dynamic). The optimal population of cooled antihydrogen may depend on the specific experiment one wants to perform. For example, there can be tradeoffs between lower *average* energy and the largest *fraction* of atoms with the lowest energy.

New cooling schemes

We will investigate schemes to further cool antihydrogen. A promising avenue for exploration is to first laser cool antihydrogen in a small volume, and then use adiabatic expansion to reach yet lower temperatures. We will also explore sub-Doppler cooling methods such as Sisyphus cooling [42].

(b) Precision spectroscopy of the 1S-2P transition of antihydrogen under various magnetic fields

Based on the *1S-2P* and *1S-2S* spectroscopy, we have reported the Lamb shift in the *2S* state of anti-H with a precision of 10 %, which is partly limited by the lineshape of the *1S-2P* transition. The laser cooling will ultimately reduce the linewidth of the *1S-2P* transition down to near the natual linewidth of ~ 100 MHz (1/10 of the one we reported in 2018). In addition, laser cooling will allow us to reduce the trap depth and the offset of the magnetic fields, such that we can precisely analyze the Zeeman effect in antihydrogen as well as the effect of the field inhomogenuity to the lineshape. Together with improved statistics, these will lead to significant improvements in the Lamb shift determination over our initial measurement. This Lyman-alpha method will be complementary to other methods proposed in this proposal such as microwave probing or a *2S-nS* measurement.

(c) Pulsed creation of the 2S state of antihydrogen

Efficient preparation of antihydrogen in the *2S* state is an important step in a number of future antihydrogen experiments, such as *2S-nS* and *2S-2P* spectroscopy, and the formation of antihydrogen molecular ions [43,44]. Our current CW 243 nm laser is able to produce some population in the *2S* state via two-photon excitation. However, in many of the future experiments, having timing information would be useful, given the relatively short (~100 ms) lifetime of the *2S* state. We are investigating various pulsed scheme to achieve efficient excitation to the 2S without the loss due to photo-ionization[45,46]. One possibility is the use of Lyman-beta (102.6 nm) radiation to drive the antihydrogen to the *3P* state, which can decay to the metastable 2S state with a 12% branching ratio[43]. With a sufficient intensity of Lyman-beta radiation, it may also be possible to induce multi-photon processes, such the STImulated Raman Adiabatic Passage (STIRAP), which could achieve population transfer with a high efficiency.

Section 5. Gravitational measurements on antihydrogen: The ALPHA-g experiment

We propose to make the first measurements of antimatter acceleration down to the 1% level of precision using ALPHA-g. Observation of the acceleration of antimatter remains a long-standing hole in empirical verification of the weak equivalence principle (WEP). While many theorists consider it unlikely that deviations between normal acceleration would exist at more than a part in 10^7, others point out that large-scale effects (10% or more) are not ruled out on the face of it[47,48,49]. General consensus is that any antimatter gravity measurement should be carried out, the results of which at any precision level will begin to constrain theory. From our perspective, ALPHA-g is an ambitious first effort, with a long-term view for higher precision measurements of antimatter gravitation.

The experiment is designed as an evolution of ALPHA's demonstrated antihydrogen trapping techniques, and addresses the systematic issues highlighted by the first proof-of-principle measurement made on the gravitational behaviour of antihydrogen[4]. In ALPHA, a trapped antihydrogen atom at a location $\boldsymbol{r}$ in the trap experiences a potential equal to:

$$\phi(\boldsymbol{r}) = \mu_B|\boldsymbol{B}(\boldsymbol{r})| - m_{\overline{H}}\overline{\boldsymbol{g}}\cdot\boldsymbol{r} \qquad \textbf{(1)}$$

where μ_B is the Bohr magneton, $\boldsymbol{B}$ is the magnetic field, $m_{\overline{H}}$ is the mass of the antihydrogen atom, and $\overline{\boldsymbol{g}}$ is the acceleration of antihydrogen in Earth's magnetic field. When antihydrogen atoms are released from the trap by lowering the confinement fields, the atoms will be systematically deflected by the gravitational force. Ground-state atoms in low-field-seeking states with sufficiently low kinetic energy are confined by a magnetic minimum. In ALPHA experiments, the simplest minimum is created by a combination of background solenoidal field to keep the population polarized, two axially-separated short solenoids ("mirrors") that create a magnetic minimum in the axial direction, and an octupole winding along the length of the trap to create a minimum in the radial direction (Figure 3). In their deepest configuration, ALPHA magnetic traps can confine atoms with energies up to about 0.5 Kelvin in equivalent kinetic energy.

In order to achieve high sensitivity to gravity, the ALPHA-g trap is oriented in a vertical direction[4,50] with the trap longitudinal direction aligned with the nominal gravity axis. With no other manipulations, antihydrogen atoms released upward by opening ALPHA would travel ~400 meters before stopping, assuming normal gravity. Therefore, the measurement consists of a controlled release of atoms achieved by balancing the top and bottom confining fields.

The gravitational potential difference over 1 meter length corresponds with a potential difference arising from a 17 gauss change in the magnetic field (Equation1). This means that with identical fields under the top and bottom confinement coils, anti-atoms will tend to fall out the bottom of the trap (under normal gravity). In a simple experiment conducted by ideally ramping our trap fields down, we would expect 70% of atoms to fall out the bottom and 30 % to

escape out the top. However, if a bias field $B_g = m_{\bar{H}}\bar{g}\,\Delta z\,/\,\mu_B$ is added to the field on the bottom of a trap of length Δz will compensate for the gravitational potential difference across the trap, atoms will leave evenly out the top and bottom. With a field of $2\,B_g$, gravity is over-compensated, and we expect the symmetric version of the first experiment. Figure 14 shows these three potentials illustrated.

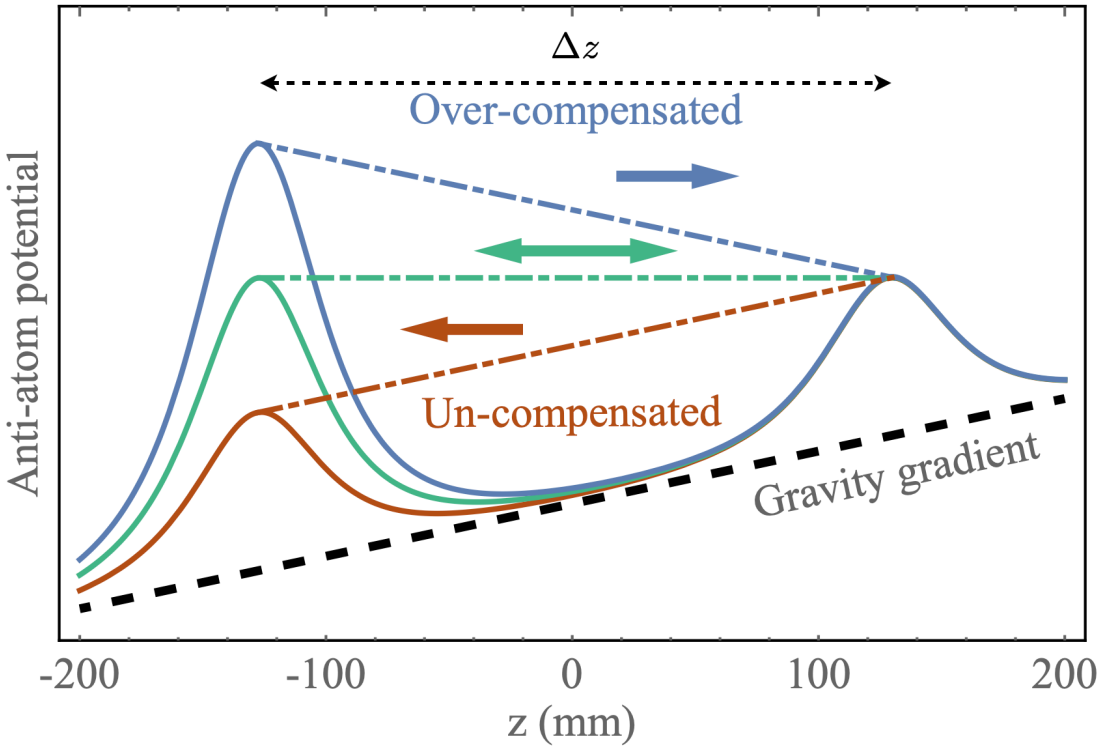

Figure 14. Illustration of the trap potential for identical top and bottom mirror coils energized to equal fields (red), gravity compensated by field *Bg* appropriate to trap length Δz (green) and over-compensated fields (blue). Arrows indicate the direction antihydrogen atoms would tend to leave the trap under the influence of normal gravitation.

In practice a measurement of $\bar{g}$ will be carried out by scanning a range of compensation curves, and measuring the relative population of particles exiting the top and bottom to the trap. The value of $\bar{g}$ can be measured by determining B_g. Figure 15 shows simulations of outcomes of different experimental protocols The precision of the measurement is determined by the confidence with which one determines B_g (the point at which the ratio of top escapees to bottom escapees balance), and the accuracy is limited by systematic effects that shift this ratio (for example, detector bias and magnetic field biases).

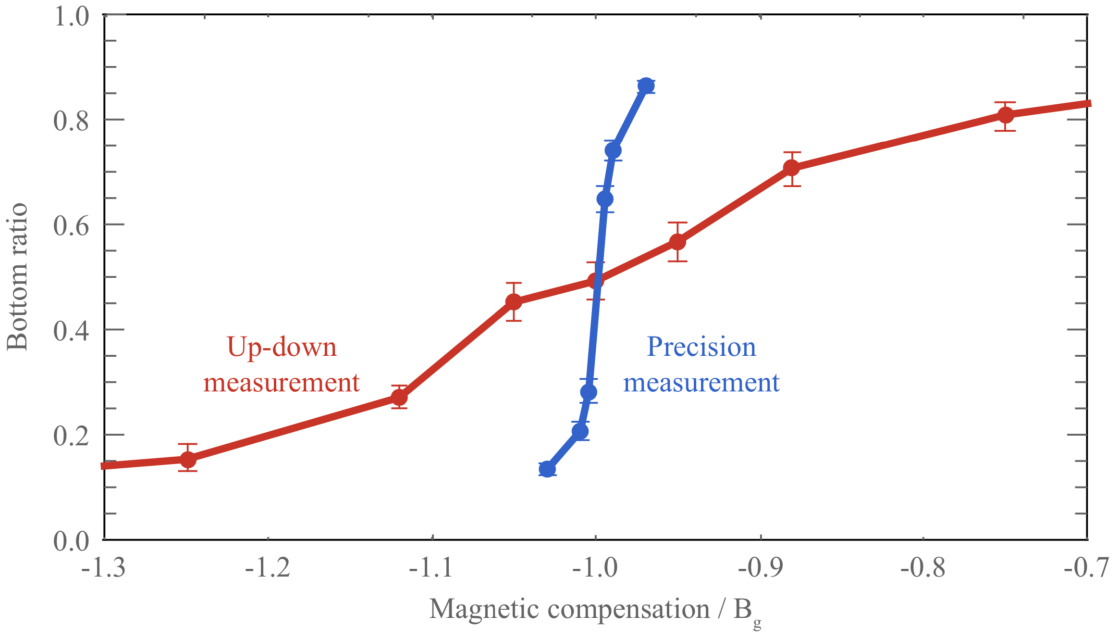

Figure 15 Simulations of the ratio of antihydrogen atoms leaving the bottom of the trap to those leaving the top of the trap. Red: a nominal measurement from a low precision atom trap, used to determine the sign of antihydrogen gravitation ("Up-down" measurement) and Blue: a gravity experiment simulation in the high-precision trap.

ALPHA-g is designed to initially achieve an experiment to test the hypothesis that antimatter and matter fall in the same direction (an "Up-down" test), while developing techniques to characterize and limit systematic effects in order to achieve a 1% measurement in the long term. The apparatus will employ ALPHA's demonstrated techniques for the production and trapping of antihydrogen produced by merging antiproton and positron plasmas. Figure 16 shows a diagram illustrating the major components of ALPHA-g; each will be addressed in turn.

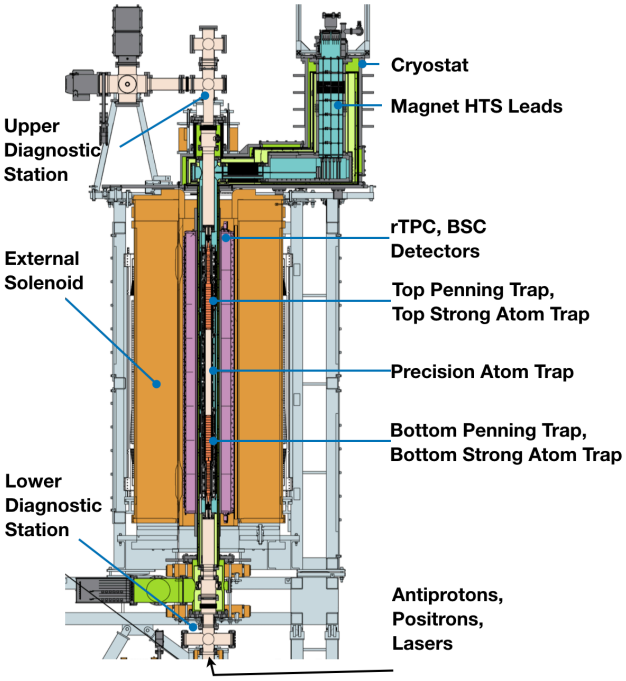

Figure 16. Diagram of the main ALPHA-g apparatus.

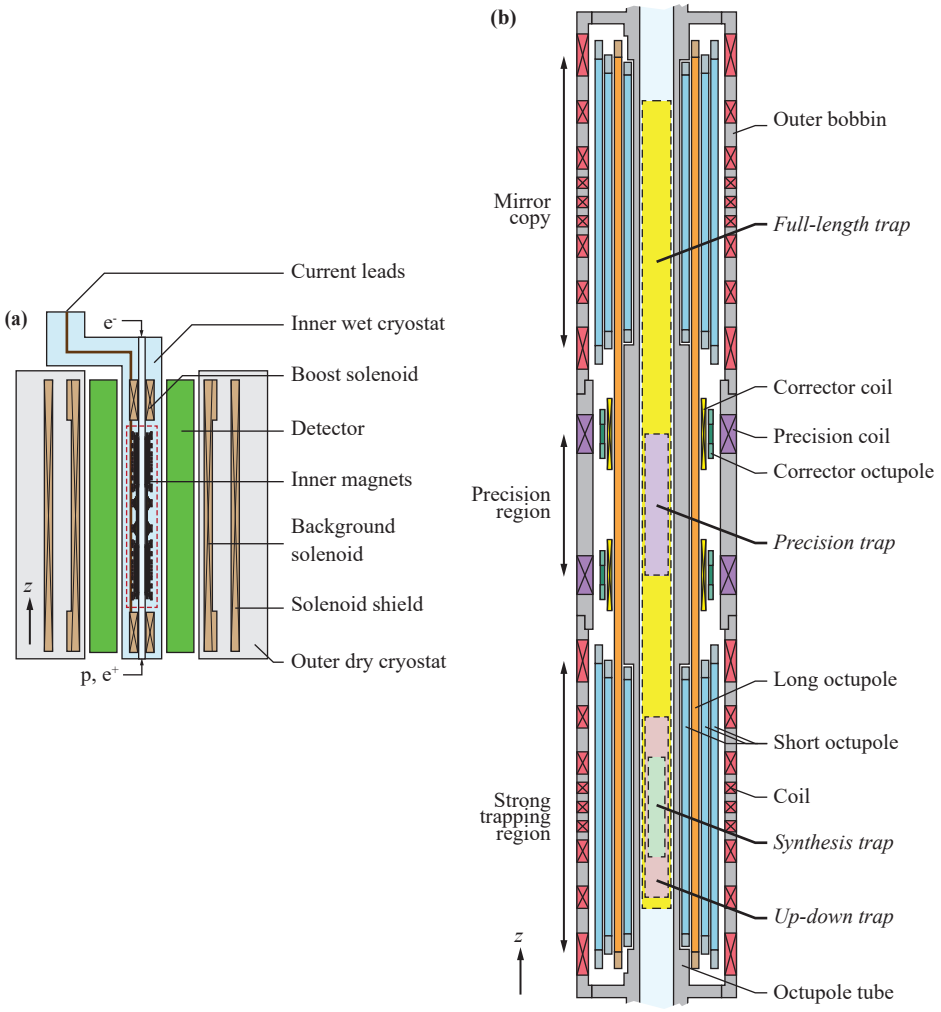

Figure 17. Detailed schematic of ALPHA-g magnet system and detector location. a) The overall ALPHA-g magnet system, including the external 1 T background solenoid, the 2 T boost solenoids used to aid in particle preparation, and the active volume of the radial TPC detector. b) The inner superconducting magnets used in antihydrogen trapping, manipulation and gravitational measurements. It consists of a symmetric upper and lower strong trapping regions used for initial antihydrogen synthesis trapping and performing Up-down measurements. The synthesis and stron traps include a series of 7 mirror coils, the outer and inner mirrors ('A' and 'G' respectively) being used for gravitational analysis. Interior coils will permit efficient adiabatic cooling of antihydrogen atoms. The central portion of the magnet system is used for performing precision (1%) measurement of $\bar{g}$, and consists primarily of two sets of matched main coils and correctors.

Figure 17 shows a schematic of the magnetic system designed for ALPHA-g. It consists of an external 1 T dry superconducting magnet manufactured by Bilfinger-Noell GmBH and used to provide the background field required for charged particle confinement and maintaining spin-polarization of the trapped antihydrogen atoms. The internal magnet system includes 22 independently controlled superconducting magnet circuits manufactured by the Magnets Group at Brookhaven National Laboratory; these are used variously for both plasma and atom trapping and manipulation. The atom trap itself is divided into three sections – two strong atom traps and one precision trap. The strong atom traps are used for initial synthesis and trapping of antihydrogen; they will also be used for performing Up-down measurements of the sign of $\bar{g}$. The central portion of

the magnet system contains a so-called precision trap. These coils include accurately-matched mirror and trim corrector coils intended to perform a determination of $\bar{g}$ precise to 1% (Figure 15 compares a simulation of an experiment in the precision region to one in an strong atom trap). Additional magnets are included to facilitate transfer of trapped antihydrogen atoms from the strong trap to the precision trap.

To achieve a particular precision on a measurement of $\bar{g}$, the magnetic fields must be controlled to a commensurate fraction of B_g (about 4 G for our traps). The two leading sources of errors in the magnet system are magnetization of the superconducting filaments in the windings due to persistent current effects and mechanical errors in the construction of the magnets. The first error is addressed in the ALPHA-g magnet system by using magnet wire that minimizes the persistent magnetization, reducing the amount of superconducting material around the precision region, and making the entire magnet system up-down symmetric, which will tend to result in the magnetization effects cancelling in the central precision trap. We expect the error to be limited to ~ 50 mG in the precision trap, which is sufficient to perform a 1% measurement. The mechanical errors are more challenging to manage, and a significant number of studies were made about possible construction errors, and the overall details of magnet and trap designs were adjusted to minimize the impact that reasonable manufacturing errors could have on performing gravity measurements.

Figure 18 shows one such study about errors in the octupole windings used in the precision trap.

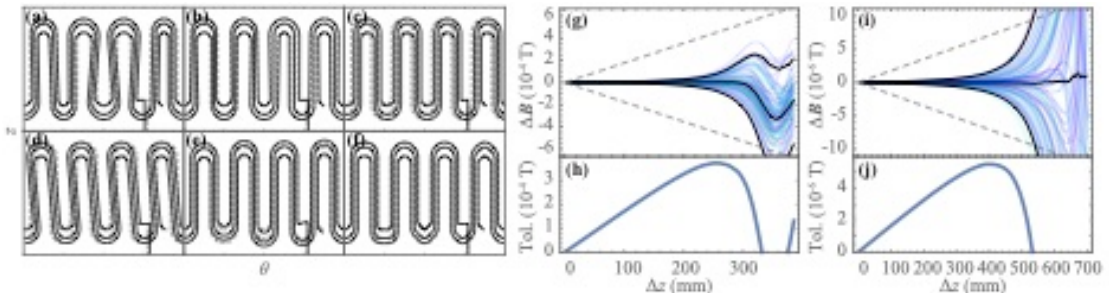

Figure 18. (a-f) Various possible deformations of an octupole racetrack pattern. (g) In blue: The difference in on-axis magnetic field between two nominally symmetric points in the strong trapping region, separated by Δz. Various curves are generated from randomly distorted octupoles. In black: The 2σ envelope and median of the spread in field asymmetry. In grey: The amount of gravity signal available in a height of Δz, expressed in magnetic units. (h) The difference between the deformation systematics and the magnetic noise in up--down measurements using traps of various lengths. (i-j) Analogous plots to (g-h) for the precision region and precision measurement. The deformation systematics is compared to 1% of the gravity signal.

Control and stabilization of the ALPHA-g magnet system is accomplished with a system similar to that employed in ALPHA-2. The internal superconducting magnets are cooled by liquid helium in the central cryostat (designed by STFC Technology, UK). Current connections to room temperature are made through high temperature superconducting (HTS) leads that are temperature-controlled by cold helium vapor extracted through normal-

conducting vapor cooled leads (American Magnetics). The control of liquid and vapor helium flow is achieved by a control system similar to that operated by us for the ALPHA-2 apparatus. Each superconducting magnet circuit is protected by active energy extraction circuits in the event of a quench. The current control system is similar to the system employed in ALPHA-2, which has demonstrated stability at the 10's of ppm level, and should be sufficient for performing Up-down measurements. We are currently developing the current control system for use in operating the precision magnet system.

In order to validate the performance of the magnet system, the fields produced over the course of trapping are to be characterized by an extensive magnetometry campaign. ALPHA has a demonstrated technique for in situ magnetometry using the electron cyclotron resonance[20], which has been routinely operated down to the 100 mG level, and demonstrated elsewhere at the 10 mG level[51] We are also planning to cross calibrate this measurement with independent magnetometers, including *in situ* cryogenic nuclear magnetic resonance probes (Figure 19) and magnetometry from Zeeman-spectroscopy of an ion species in the trapping volume[52]. Presently, cryogenic NMR probes are demonstrated at the gauss level with room temperature probes in the experiment operating at the 5 mG level. Required precision may also be achievable by an adaptation of new flux loop techniques conducted by the CERN Magnet Measurement group. For measurements of the fields on the strong atom traps for use in the initial Up-down campaign, the ALPHA-g penning trap is designed to co-locate plasmas directly under each relevant trap magnet, particularly those on the extreme ends (Figure 20).

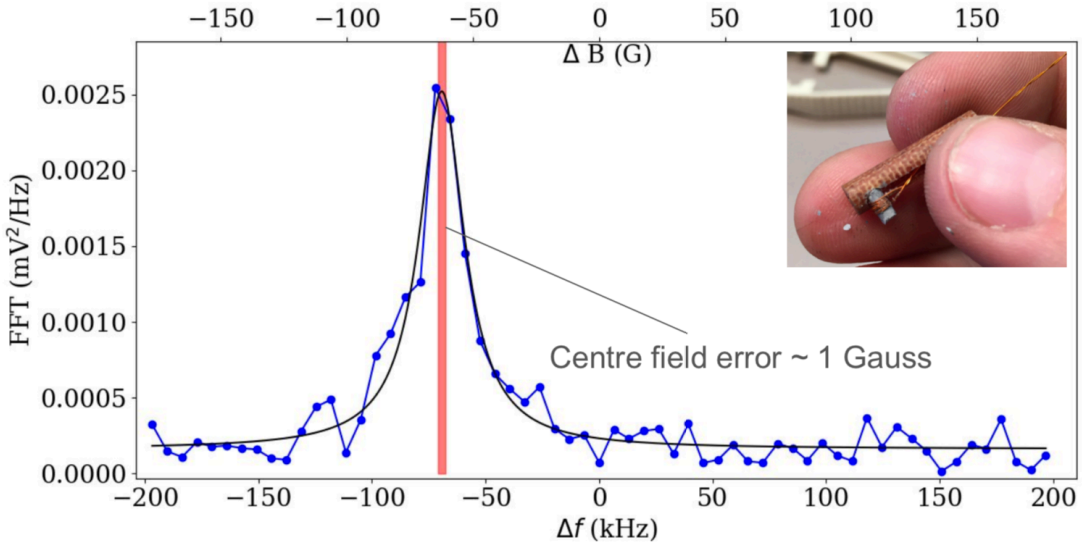

Figure 19. Prototype of a cryogenic NMR probe and its response in a nominally 1 Tesla field, operating at 15 K in ALPHA-g.

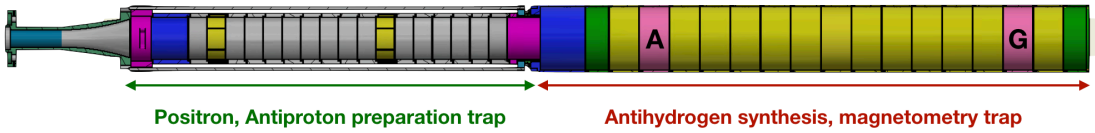

Figure 20. Schematic of a single ALPHA-g penning trap. The trap consists of two regions: the preparation trap is used for preparing antiproton and positron plasmas for use in antihydrogen synthesis, and sits under the boost solenoid, allowing leptons to benefit from additional cyclotron cooling at 3T. The synthesis and magnetometry trap is located under a strong magnetic trap. Electrodes are sized to enable symmetric ECR measurements under mirrors A and G for use in an Up-down gravity measurement.

ALPHA-g determines which side an antihydrogen atom escapes from a given atom trap by observing the annihilation with the wall once the atom escapes. A detector system consisting of a 2.3 meter long radial time projection chamber (rTPC) with a surrounding barrel of scintillating bars (BSC) times and reconstructs antiproton annihilations. The rTPC functions by accelerating ionization electrons which drift outwards under the influence a radial electric field crossed with the 1 T background solenoidal field (Figure 21), and are collected by anode wires and readout pads. Events are reconstructed from the time history of charge readout from the rTPC's 256 wires and 18,432 pads on the outer cathode. The expected resolution for vertex reconstruction is ~ 5 mm in *z*, 9 mm in *r*, and about 18 degrees in azimuth. This is more than sufficient to meet the required resolution in *z* for a 1 % measurement of gravitational acceleration, which is on the order of several centimeters[53] (Figure 22).

The outer BSC detector consists of 64 scintillating bars running the length of the rTPC, instrumented with silicon photomultipliers on either side. With an intrinsic time resolution of < 300 ps, the BSC is able to distinguish events originating from within the detector volume (likely antiproton annihilations) from cosmic rays. The ALPHA-2 apparatus currently uses "cuts-based" analysis and boosted decisions trees to reduce the cosmic background rate by factors of 200 and 2000 respectively. The addition of the BSC as a cosmic veto detector should suppress this by a further factor of 100. With a cosmic background rate of approximately 7 Hz, this suppression factor will allow easy distinction between annihilation events and cosmic events, which would otherwise reduce the sensitivity of a gravity measurement.

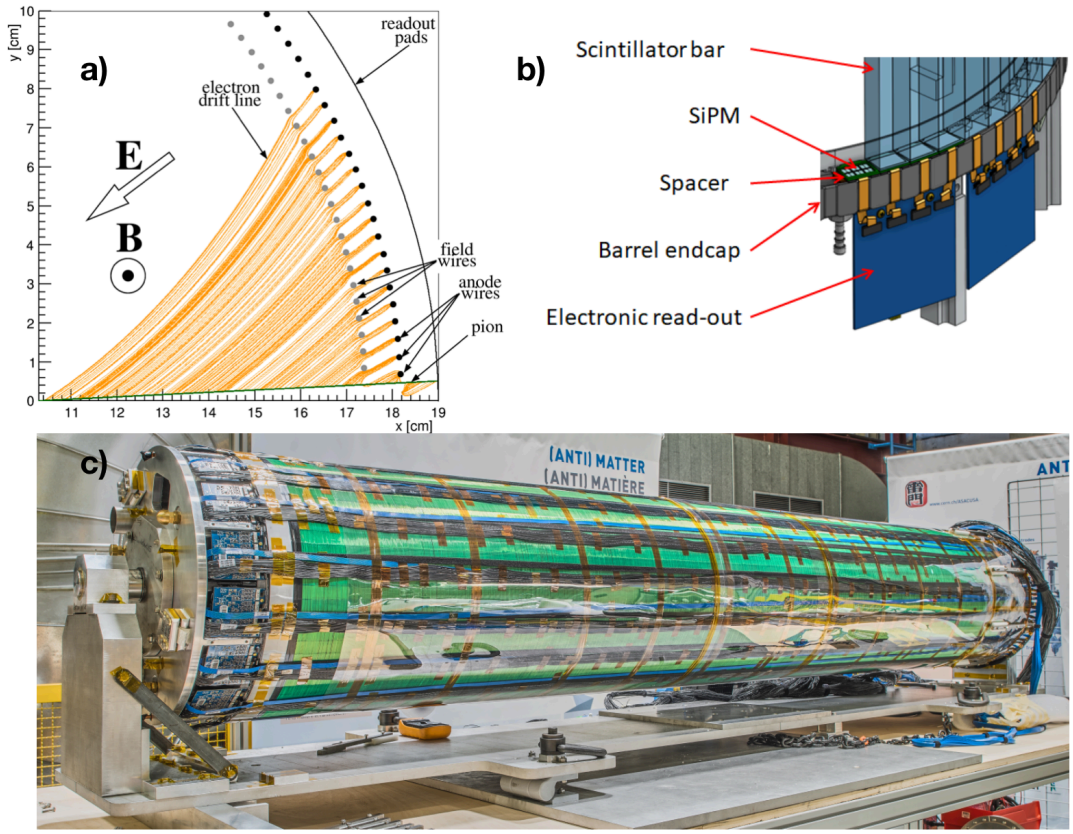

Figure 21 ALPHA-G detector technologies. a) Garfield[54] simulation of an antiproton annihilation pion track and consequent ionization electron drift tracks through the active volume of the rTPC. b) one end of the BSC detailing the silicon photomultiplier readout at the end of the 2604 x 243 x 223 mm scintillating bar. Identical readouts are installed on opposite ends of the bar. c) External view of the BSC prior to installation in ALPHA-g at CERN (2018).

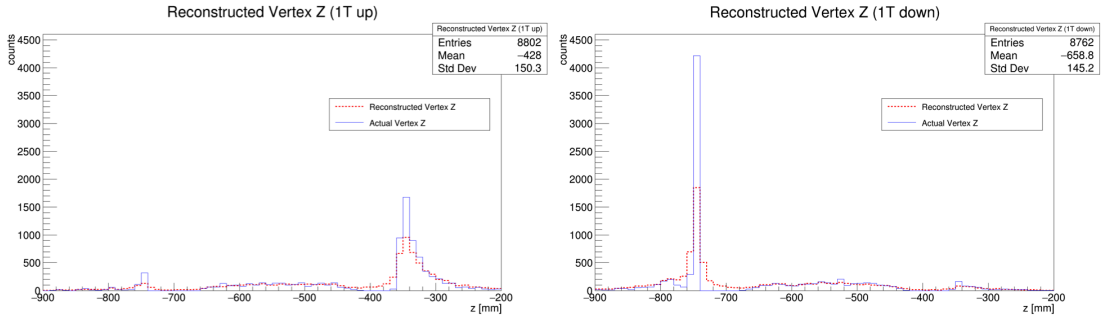

Figure 22. Early Monte-Carlo simulations of Up-down experiments in the rTPC showing equivalent efficiencies for counting antihydrogen atoms escaping entirely up or down from the lower strong atom trap [see reference [53] for details].

ALPHA-g is designed to operate in a manner similar to all other ALPHA experiments to date. The addition of a new beamline with a special interconnect magnet between ALPHA-g, ALPHA-2, and the positron accumulator (Figure 24)

allows the new experiment to be fed with antiprotons and positrons in a manner similar to the operation of ALPHA-2. With a suite of equivalent plasma sources, diagnostics, Penning traps and control systems, we anticipate producing trapped antihydrogen in a manner commensurate with existing ALPHA experiences. Additionally, the experiment has been designed to enable on-axis optical access through the experiment. We plan to integrate a Lyman-α laser system for use in laser cooling (Section 4) and will be able to integrate beryllium laser cooling and diagnostics for use in antihydrogen production and magnetometry (see Section 7).

ALPHA-g Status

Construction and installation of the ALPHA-g experiment began at the end of May in 2018 and was completed at the ALPHA zone by the end of the 2018 beam period of the AD. In addition to significant infrastructure upgrades to the ALPHA zone (water, electrical, mechanical), this included the new ALPHA-g beamline and main apparatus and accompanying control and service hardware. The main ALPHA-g apparatus broadly consists of the following components: the Penning traps and their diagnostics, the cryostat and magnet system, the vertex detector and the external solenoid. Initial commissioning of all major components of the experiment was largely completed by the end of the 2018 beam period.

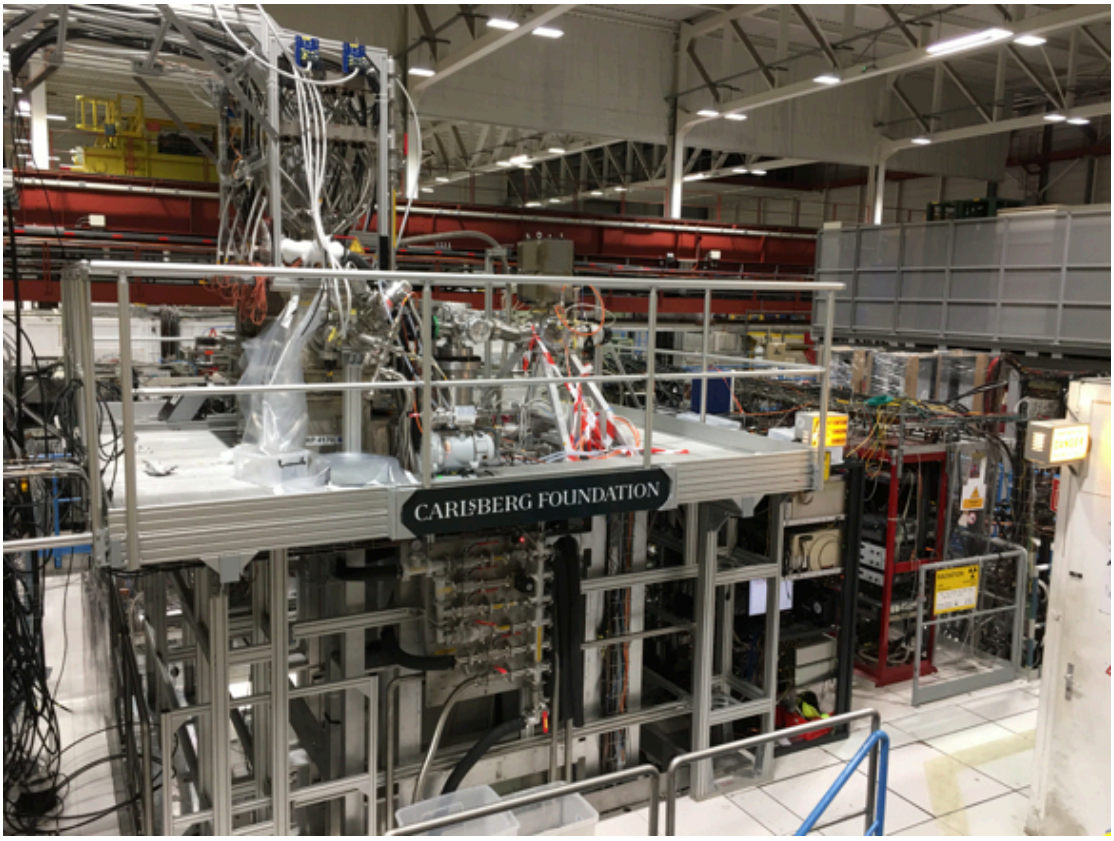

Figure 23 Photo of the top levels of ALPHA-g, as installed in the ALPHA zone, November 2018.

ALPHA-g Beamline and Penning traps

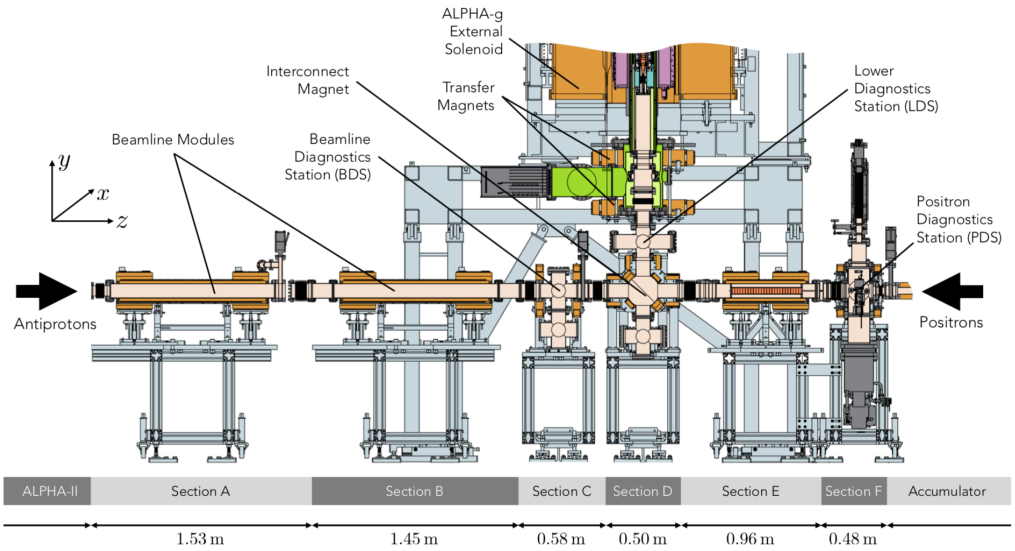

Figure 24. Diagram of ALPHA-g beamline as installed (2018).

The ALPHA beamline was installed from the end of May and commissioned for use by ALPHA-2 in June of 2019. Diagnostic stations such as that shown in Figure 25 were commissioned to image particles at various points along the beamline and up into ALPHA-g. Positrons were successfully transported to ALPHA-2, enabling a successful physics campaign on that apparatus (see Sections 1, 4). Once the main ALPHA-g components arrived, an intervention to install the upper vacuum system and interconnect was performed, and both positrons and antiprotons were efficiently transported around the interconnect and into ALPHA-g.

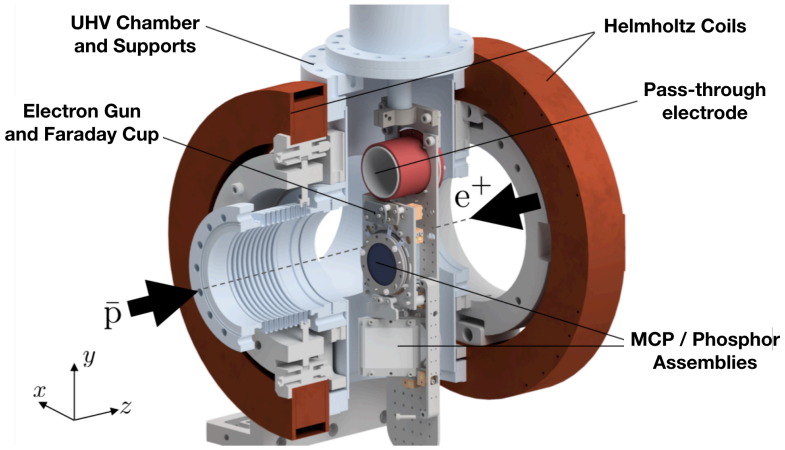

Figure 25. Diagram of a dual-facing diagnostic station for use in ALPHA-g. A number of diagnostics are installed on the length of a linear translator. Each station is equipped MCP / Phosphor screens facing are used to image or measure current from charged particles directed to the diagnostics station. Electron guns face in both stations are utilized to load electron plasmas in ALPHA penning traps, as well as for alignment and tuning of beamline elements. A pass-through electrode allows particles to transit through the station, and can be biased for bunching and lensing operations. A set of Helmholtz coils is used to tailor the magnetic field around the station in order to optimize particle imaging and plasma production.

Images of positrons and antiprotons were made as particles passed through the interconnect and into ALPHA-g (Figure 26). By systematically varying currents in the interconnect magnet, steering points could be matched against simulation, and particle steering onto the axis of the ALPHA-g Penning traps was achieved with over 90% of particles arriving at the trap.

Only the bottom Penning trap was installed in ALPHA-g during the 2018 run period. Once steering around the interconnect had been achieved, trapping positrons and antiprotons was readily established. We were able to begin work on preparing plasmas for antihydrogen production, including cooling of antiprotons (Figure 27). We attempted to form antihydrogen, and while we had not achieved the level of finesse needed to produce the anti-atoms in the last two weeks of the run, we are confident that there are no road blocks to achieving this milestone in ALPHA-g. As we have emphasized, operation of ALPHA-g involves no new techniques that need to be developed. The essential processes have been highly developed through years of operation with ALPHA and ALPHA-2.

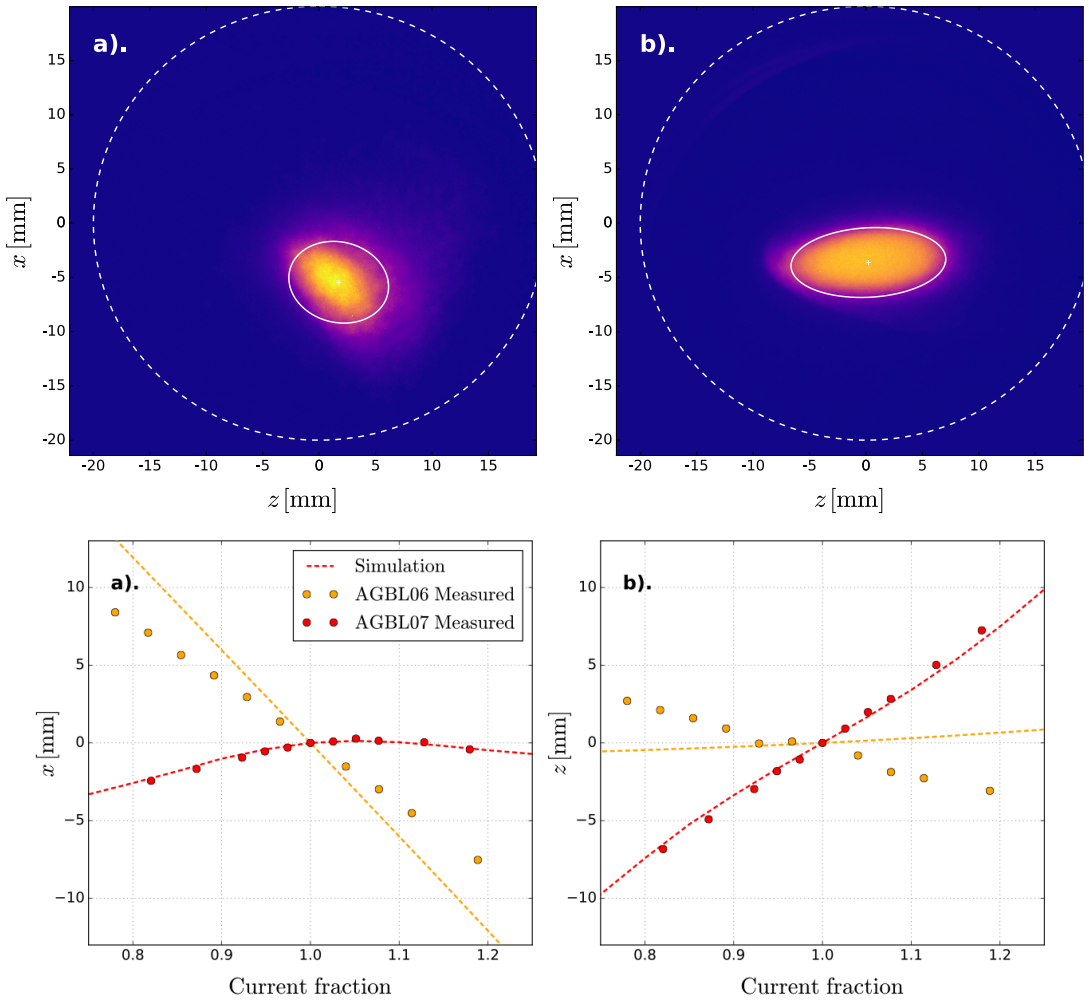

Figure 26. Top: Images of a) antiprotons and b) positrons taken by the MCP/Phosphor screen on the Lower Diagnostic Station after transit around the interconnect. Bottom: Steering curves generated for a) antiprotons and b) positrons of particles headed into ALPHA-g.

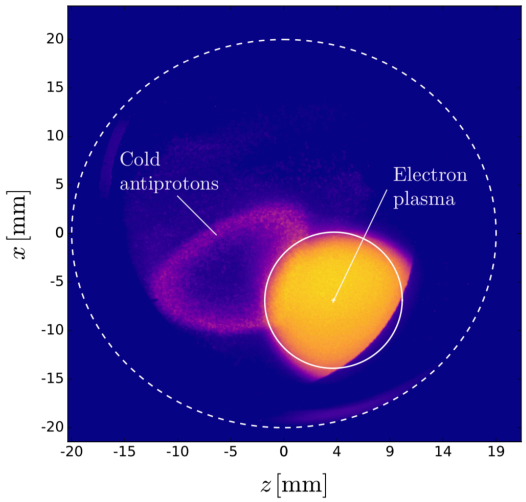

Figure 27. MCP image of an electron and a centrifugally-separated antiproton plasma extracted from the ALPHA-g bottom Penning trap at 1 T after 50 seconds of electron cooling of the antiprotons. (2018)

ALPHA-g Magnets and Magnetometry

In order to commission ALPHA-g at CERN in 2018, only the bottom strong atom trap and ancillary magnets were installed and instrumented for the run. Due to the lengthy nature of the task, commissioning the magnets for high-current operation was not completed until after the antiproton beam time had ended. However, we were subsequently able to verify that the installed magnets were operational at their nominal set-points. This was an important step for verifying the functionality of the new choice of superconducting wire made for the ALPHA-g magnets.

We also carried out a brief ECR campaign to align the bottom Penning trap with its associated strong atom trap. With the first magnetometry system operating in ALPHA-g, we were able to verify the mechanical registration of the two structures to within 0.3 mm. While there is still a lot of work to be done characterizing the ECR measurement in the high fields intended for use in the experiment, this gives us confidence that this trap will perform correctly for diagnosing an Up-down measurement.

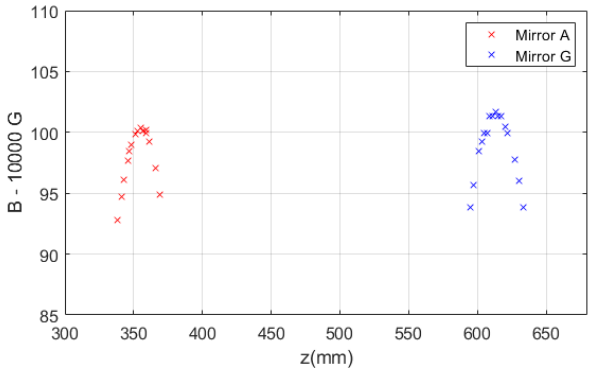

Figure 28. ECR scans of fields generated by low-current energization of mirrors A and G (bottom strong atom trap).

ALPHA-g Detectors

The ALPHA-g rTPC and BSC were both constructed and commissioned by members of the Collaboration and TRIUMF. Cosmic detection and reconstruction were demonstrated before the detectors had shipped from Canada. During the beam period, with the detector installed in ALPHA-g, and antiprotons in the bottom Penning trap, the first reconstructions of antiproton annihilations were made (Figure 29).

During commissioning, once we were able to trap antiproton plasmas, we could begin a survey of the rTPC's spatial reconstruction efficiency. Figure 30 shows the results of a few measurements in which antiproton plasmas were held and moved between a few electrodes in the bottom Penning trap. While these results are very promising and complete the first round of tests on this new detector, more work will have to be done in order to better characterize the background due to cosmic rays and to improve the accuracy with which the annihilation location is identified.

In order to maximize the offline analysis output, the careful mapping of the magnetic field must be exploited, especially in the regions near the edges of the detector where the homogeneity of the field is poor. For this reason, the rTPC is endowed with a series Hall probes located on the outer cylinder and with its own laser calibration system, which provides important information about the drift time of the electrons. To make the most proficient use of these devices, more automated tools must be developed in order to incorporate their measurements in the physics analysis.

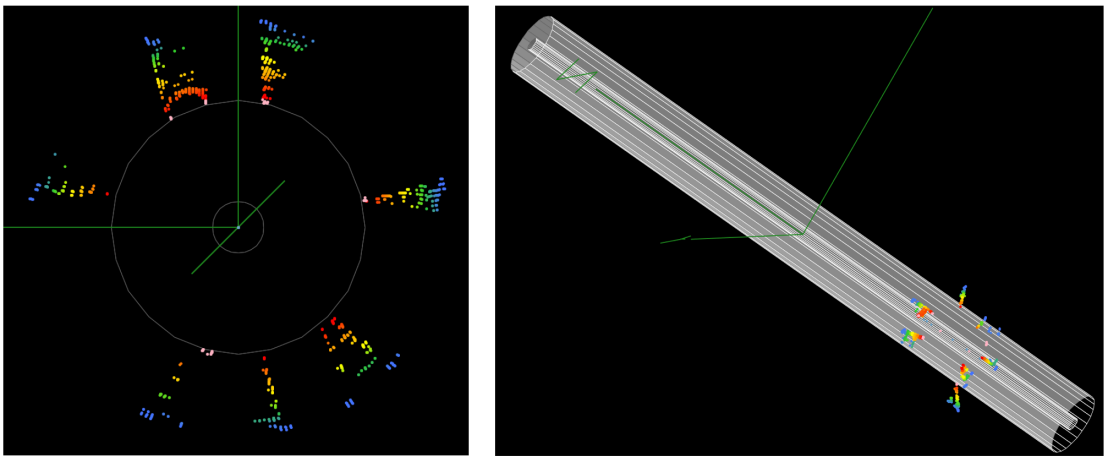

Figure 29 Reconstruction of a single antiproton annihilation event in the ALPHA-g rTPC. (2018)

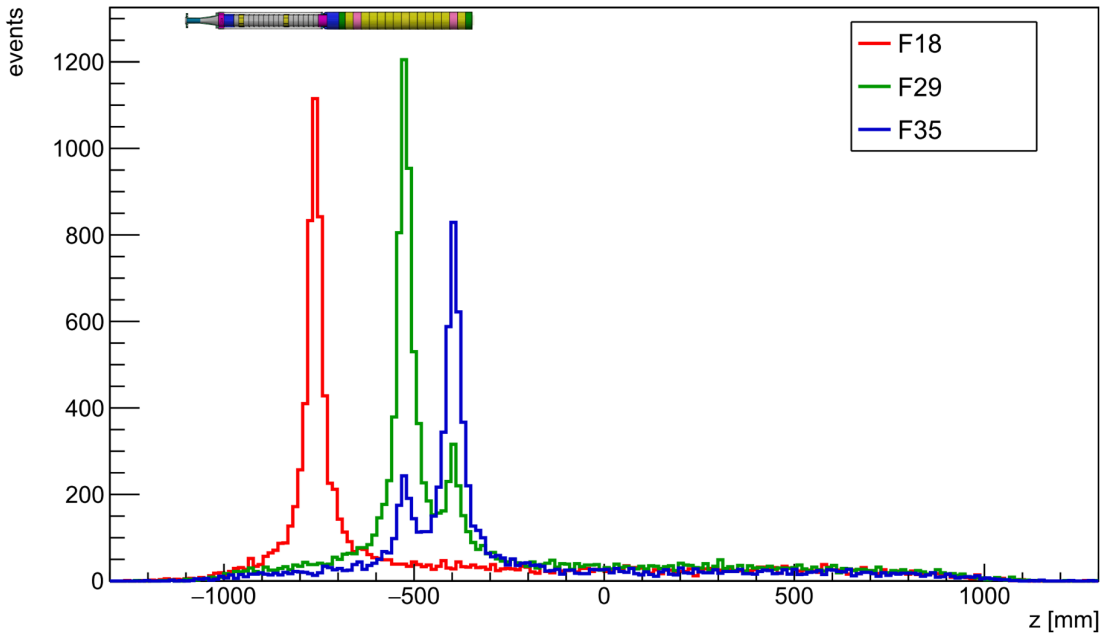

Figure 30, Reconstructed vertical position of antiproton annihilations from an antiproton plasma held in electrodes 18, 29 and 35 in the ALPHA-g bottom penning trap. Penning trap included for scale.

ALPHA-g Measurements and Milestones

After a successful commissioning run in 2018, we have been upgrading and maintaining ALPHA-g in preparation for the return of beam in 2021. The most significant aspect of this work is the construction and installation of the remaining magnets (for the second strong atom trap and analysis region) in the internal magnet system. This activity necessitated the complete disassembly of the cryostat. Magnet fabrication is presently underway at Brookhaven National Lab, with work scheduled for completion by the end of 2019. Additionally, the rTPC has been returned to TRIUMF for servicing after this initial run. We anticipate re-assembly and re-commissioning of the ALPHA-g apparatus in H1 2020. With the apparatus on the beamline, we will focus the remainder of LS-2 developing particle manipulations and diagnostics anticipated for use in the first gravity campaign. This will naturally include the first magnetometry campaign focused on performing an Up-down measurement.

We plan to begin Run 3 with the performance of an Up-down measurement in both strong traps, and characterize systematics that would influence performing a 1% measurement. We will develop techniques to adiabatically and laser cool antihydrogen atoms in ALPHA-g. This will naturally lead to developing transfer of antihydrogen form the strong to the precision trap. We will then directly evaluate experimental protocols carried out from the precision trap. In parallel, we will continue to refine and develop magnetometry and magnet control as needed to support this effort, with the ultimate goal of performing a 1% or better determination of $\bar{g}$ by the end of 2024.

ALPHA is committed to performing the highest-precision measurements possible with antimatter to compare with matter. Precision gravity measurements on matter are performed at sub-ppt levels. While it is not clear at

this time what the ultimate limit of the ALPHA-g apparatus will be, it is likely that a different approach will be necessary to reach significantly higher precision. We are considering an atom interferometry technique which would be compatible with an ALPHA-g-like apparatus[55]. Other schemes include creating a separate antihydrogen fountain, see Section 7. In all cases, it will be useful to gain operational experience with the existing ALPHA-g experiment before committing to any particular strategy on this front.

Section 6. ALPHA operations with ELENA

ELENA and the AD

The ELENA upgrade to the AD complex changes the antiproton delivery to experiments such that the kinetic energy is reduced from 5.3 MeV to 100 keV, and instead of a single bunch of ~200ns length delivered every ~2 minutes, four bunches with μs separation will be delivered with a similar length and transverse emittance as before. Historically the AD beam per-shot intensity is about 30 million antiprotons, thus, assuming 100% efficiency of deceleration in ELENA, each of the above four bunches from ELENA will contain around 7.5 million antiprotons. At 100 keV, the ELENA beam will be delivered by electrostatic beamlines, that allow fast switching such that each of the four bunches can (and will) be sent to separate experiments.

Since its start up for physics in 2000, the AD has delivered beams to the experiments following a shift schedule. This approach was driven, at least in part, by the observation that switching beam between experiments is comparatively cumbersome due to hysteresis in magnets, among other issues. It was certainly not possible, with the AD, to send every consecutive spill to a separate experiment. Therefore the AD beam was distributed to separate experiments in 8 hour blocks. In 2000 only three experiments were active, so each experiment had 8 hours per day for the season, only the timing of the block changing to average out (in)conveniences of running a given time of the day. In recent years, about five experiments have been active, leaving each experiment without any beam for two weeks out of every five. This unavoidable mode of operation necessarily led to lower than optimal exploitation of the beam, in that, for example, some experiments during some phases accumulated antiprotons for say 30 minutes by taking every spill, and then they blocked the beam to reduce background from the beam. Other experiments, such as ALPHA, might in some periods use every single spill, whereas in other periods, use only every second or every third, due to the duty cycle of the experiments being performed. ELENA allows all experiments to profit maximally from the antiprotons produced at CERN in that the four bunches that circulate in ELENA at ejection energy can be directed to four different experiments. Thus, if only four experiments are active, every experiment can receive a spill on every accelerator cycle (~2 min) all 24h. With more experiments, every experiment will be guaranteed a spill every ~4 min, but due to the varying duty-cycles and levels of readiness it seems likely that most experiments will, when they are operational, experience constant

beam availability. This is a massive improvement over the past. Time with beam access is of the essence here, as historically we spend by far most of our time (>80%) on development of particle manipulations in the most general sense, whereas integrated intensity is much less of a factor for progress - very much in contrast to typical particle physics experiments. For our program planning in this proposal we are thus assuming near continuous access to antiproton beam as explained above during beam periods for the foreseeable future.

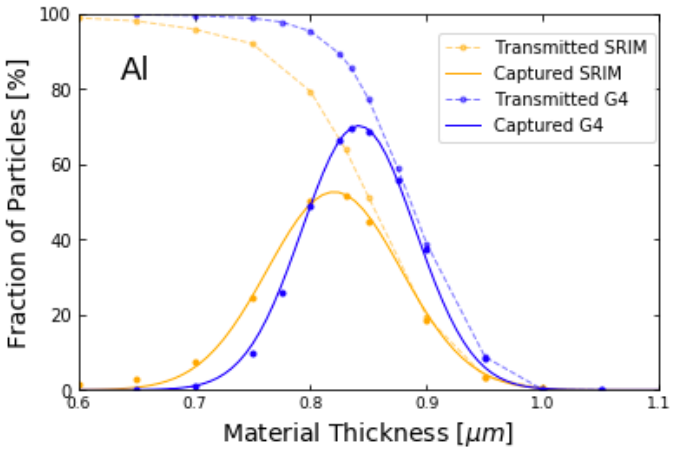

Figure 31. Calculation of the fraction of protons captured as a function of aluminium foil thickness for 100 keV protons. The two calculations use different models as indicated in the legend. For antiprotons the Barkas effect has to be included[56,57], which increases the thickness by about 30%.

The lower intensity per bunch from ELENA compared to the AD will be offset by the significant reduction in degrading material needed to stop the 100 keV beam compared to the former 5.3 MeV beam. As shown in **Figure 31**, the degrading efficiency of antiprotons into our trap could be as large as 70%, significantly above the current efficiency of around 1% for 5.3 MeV antiprotons. Thus, even with a single ELENA bunch delivered every 4 minutes, the number of antiprotons available for our experiment will increase by almost two orders of magnitude, including both the more efficient degrading and the improved duty cycle. However, to achieve this we are implementing some changes to our apparatus as described in the next section.

Modifications to ALPHA

The current ALPHA apparatus was described in the introduction to this proposal. A key feature is the modular structure that was introduced with the ALPHA-2 upgrade done during the CERN LS-1. During this upgrade antiproton capture was relegated to a specialized trap called the catching trap (CT) and antihydrogen synthesis to a separate device. This was done both in anticipation of ELENA and as a way to improve access to and performance of the antihydrogen synthesis and trapping system. By separating antiproton capture from the antihydrogen operation, modifications necessary to allow for capture of antiprotons from ELENA will only need to be done on the CT.

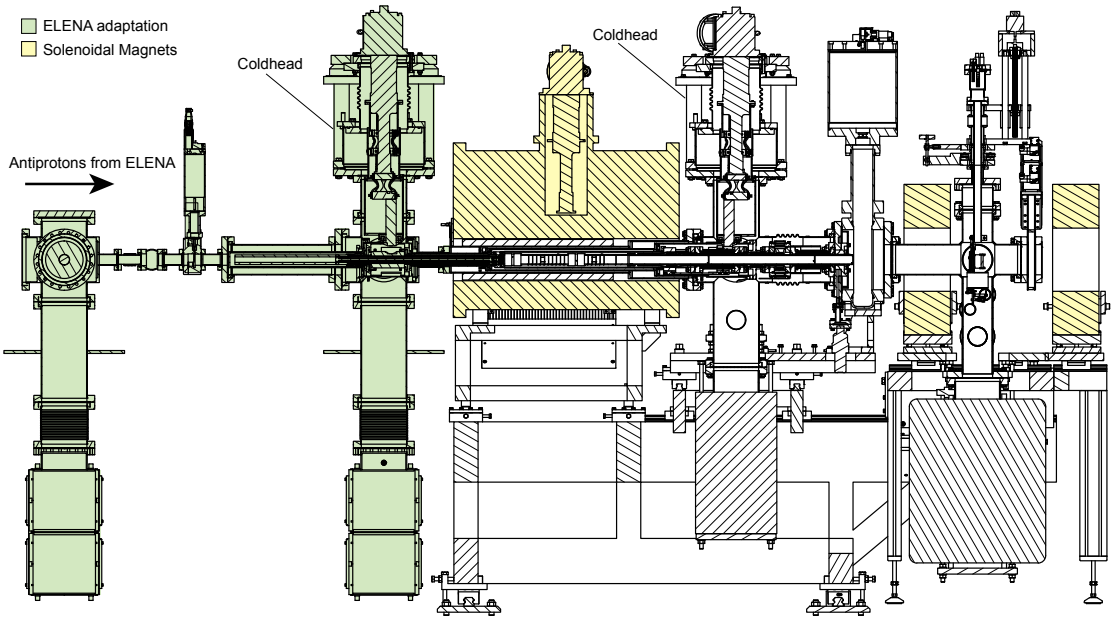

Figure 32. Side view of the ELENA-adapted version of the CT. The sections to be modified are highlighted.

As shown on **Figure 31**, the foil thickness required to degrade the ELENA beam is on the order of a micrometer. In the current CT, by contrast, about 216 microns of aluminium is required. As good vacuum ($<10^{-12}$ mBar) is crucial for operation with antiparticles, the existing system is cryogenic and not open towards the AD beamline, where typical vacuum was of order 10^{-9} mBar. Additionally, the exact thickness of the foil needed cannot be calculated accurately as the knowledge of antiproton stopping power at these low energies is limited. The planned upgrade, shown in **Figure 32**, consists therefore of (a) opening up the AD-facing end of the CT, adding additional pumping and a cryo-cooler to make the vacuum performance compatible with the ELENA beamlines and to maintain the performance for caught antiprotons, and (b) installing an exchangeable foil setup, that allows us to quickly exchange foils until the optimum thickness has been found. Rotatable foils are not possible due to the large rotations required and the large cyclotron radii of the slowed particles in the magnetic field. The geometry also makes them non-viable. Once the correct foil thickness has been installed, we do not expect any further interventions on this system for several years. Indeed, we have not aired up the existing CT for more than five years, demonstrating the robustness of the approach.

ALPHA operational strategy

A typical current operational cycle, consisting of repeated cycles of capture and preparation of antiprotons from the AD, capture and preparation of positrons from our positron accumulator, mixing and trapping of antihydrogen is illustrated in Figure 33.

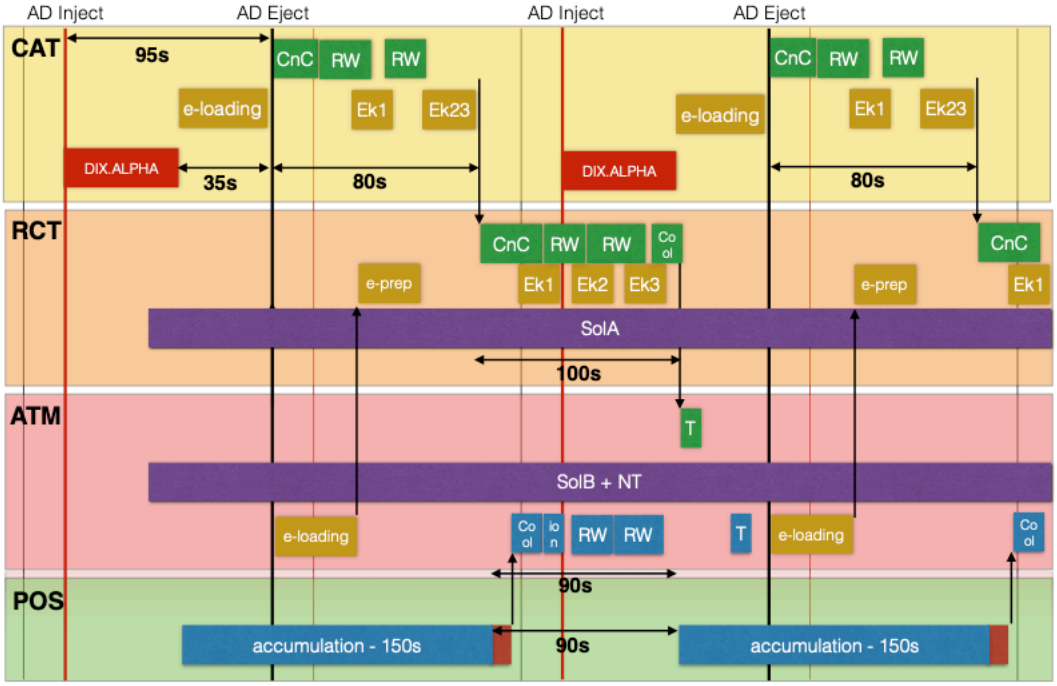

Figure 33 Typical antihydrogen stacking cycle showing the activities of the Catching Trap (CAT), the Recatching Trap (RCT), the Atom Trap (ATM) (that together form the Spectroscopy Trap) and the positron accumulator (POS). Note that the full complement of neutral trap (NT) magnets and capture solenoids (SolA, SolB) is continuously energized from the start. The diagram is illustrative of the overall timimg; we will not discuss the detailed manipulations here.

The various preparation times, dominated by the need to carefully prepare the various particle species for the correct cloud dimensions, particle number and temperature, result in our using every second shot from the AD, such that we synthesize and trap a batch of antihydrogen about every 4 minutes (two AD cycles), as shown in Figure 33.

From 2021 we expect to be able to run both ALPHA-3 (RCT and ATM above), an upgraded version of ALPHA-2 (the current apparatus) and ALPHA-g (the new vertical addition) in a similar fashion to the scheme above. Both machines will be equipped with systems for *1S-2P* laser-cooling (the same primary laser-system, separate final 121 nm generation) and potentially also with Be^+ driven sympathetic cooling of positrons (Section 7), but the latter only after confirmation of the expected increase in trapped antihydrogen. Both systems require a lot of development work with all particles species, and simultaneous running (or nearly so) will allow for full exploitation of the 24/7 availability of beam with ELENA. ALPHA has been running 24/7 shifts for many years, allowing great progress to me made on many techniques that didn't necessarily require antiprotons. The 16 hours of offline preparations permit optimal use of the limited antiproton time, and are key to our successes and to the reproducibility of our measurements. We intend to continue this successful strategy with ELENA. In 2021, the top priority will be to do a first measurement of the antihydrogen gravitational to inertial mass ratio, with the newly commissioned ALPHA-g, but we intend to have ALPHA-3 fully ready to perform

improved spectroscopy on the *1S-2S* transition as well. Any down or development time in one experiment is to be exploited by the other, thus ensuring maximum physics output.

Initially we expect to need to use up to a month to first adapt fully to ELENA, the timescale being driven by the need to exchange the degrading foils to find the optimum thickness. This should allow up to 5 million antiprotons to be caught from each ELENA spill. These can, as confirmed in the initial tests in 2018, be transferred to the Spectroscopy Trap or directly to ALPHA-g (ballistically moving through the Spectroscopy Trap, see the arrangement in Figure 2). There may also be delays associated with the commissioning of the new beamlines between ELENA and the experiments.

Next, a number of development projects will take place, some in parallel, and some in series:

a) Achieve full parametrical control of both positron and antiproton plasmas in ALPHA-g, followed by antihydrogen synthesis and trapping. This could initially be done with antiproton numbers reduced to ~100'000 in order to be able to directly apply the techniques and parameter ranges developed in the Spectroscopy Trap.
b) Achieve full parametrical control of a full ELENA load of antiprotons (5 million) in the CT. This will require new electron plasma parameters and subsequent combined manipulation of mixed antiproton/electron plasmas, currently optimized for ~200'000 trapped antiprotons.
c) Develop antihydrogen synthesis in both the Spectroscopy Trap and ALPHA-g that exploits the full batch of cold antiprotons that can be achieved from an ELENA antiproton spill. This will require new electron, positron and mixed plasma developments.

Once these tasks are completed, both ALPHA-3 and ALPHA-g will be fully operational and able to exploit the full ELENA intensity, and we will have full flexibility to switch between them at our leisure. As pointed out above though, the priority will be given to making a first gravitation measurement, for which only point (a) above needs to be accomplished.

Longer term, we envisage possibly stacking more ELENA spills, or better, filling both antihydrogen traps simultaneously with alternating ELENA spills (the preparation for synthesis in the traps is the bottleneck in our timing), as accumulation of the neutral antihydrogen is far more straight forward than accumulating antiprotons.

CERN Resources Required

For the operations envisioned above we expect CERN to continue basic delivery of power (<300kW), pressurized air, cooling-water and room temperature gasses. We will of course continue to need liquid helium. The current consumption of the Spectroscopy Trap (which includes two cryostats, one for the atom trap and one for the main Penning trap solenoid) is about 19L/h, thus with current deliveries about 9 dewars of nominally 500L per week. We expect

ALPHA-g to consume a similar amount of liquid helium as the improvements in the cryostat are off-set by the increase in the number of independent magnets (and therefore leads) required to make the gravitational measurements. The Spectroscopy Trap has 16 HTS leads, ALPHA-g has 34.

A total delivery of 18 dewars per week is a large logistic exercise, and all the mechanical/crane activity entails some risks (though nothing untoward has ever happened at the AD in this regard in 20 years of running). This is also beyond the current capacity available to us. It is a credit to the helium service and to the transport teams that this system has functioned very well over the years and never adversely impacted our ability to do physics. We would therefore like to take this opportunity to strongly encourage CERN to continue the plans to implement a distribution system for liquid helium in the AD hall, and in addition we believe it would be pertinent to install a dedicated AD helium liquefier to ensure a simplified service. Such an upgrade to the facility will ensure our ability to fully exploit the potential created by the advent of the ELENA machine. It is our goal to be able to operate both ALPHA-3 and ALPHA-g essentially continuously during the AD physics runs – excepting those times when stray fields from one device might compromise the measurements in the other. In any case, the internal portions of both machines should be kept cold at all times.

As described earlier, ALPHA is in desperate need of increased laboratory space for both preparation and development of experimental setups, as well as storage for equipment, spares, etc. The challenges of high precision metrology for antihydrogen spectroscopy demand a new room in building 393 to house our atomic fountain clock. Space inside the AD hall for new laser equipment and other apparatus would also be of interest if it becomes available.

Section 7. Future ALPHA Developments

Laser-cooled Beryllium ions in ALPHA

As pointed out previously, the arrival of ELENA is expected to improve our ability to do antihydrogen physics in two different ways, reiterated here:

a) The availability of four bunches at low energy every two minutes, will allow for servicing of either four simultaneous experiments every two minutes, or in a model where more experiments are taking beam, eight experiments every four minutes.
b) The estimated 5-7 million antiprotons at 100 keV in each spill from ELENA, is expected to allow dynamic trapping of around 2-5 million antiprotons per spill - more than an order of magnitude above what is currently possible.

Looking at how ALPHA has been operating over the last 14 years, the most immediate effect will come from (a), as essentially all current procedures can be continued as is, increasing the accumulated antihydrogen production by a factor 4-5 from duty-cycle considerations alone (we received about 20-25% of the

beamtime in the last few years). Additionally, the increase in the total time antiprotons are available will increase the time for development, which historically takes up more than 80% of ALPHAs experimental time. This additional time will be crucial to move towards exploiting (b), as the manipulations leading to successful antihydrogen synthesis and trapping are sensitive to the exact particle numbers, and years of optimization have gone into our current, most efficient scheme[58]. Potentially of course, we are looking at a two order of magnitude increase in the number of antihydrogen atoms trapped per unit time.

However it is not obvious to what degree increased numbers of antiprotons will translate into increased antihydrogen production. As an example of an obstacle to overcome, we can mention that more positrons will be needed. This may lead to a radially larger positron plasma (synthesis is sensitive to the density, which one may therefore want to keep constant). A larger positron plasma could interact with the non-rotationally symmetric magnetic fields in the antihydrogen trapping region, which can in turn lead to both increased temperatures (lower antihydrogen production cross section) and losses[59,60,61,62,63,64].

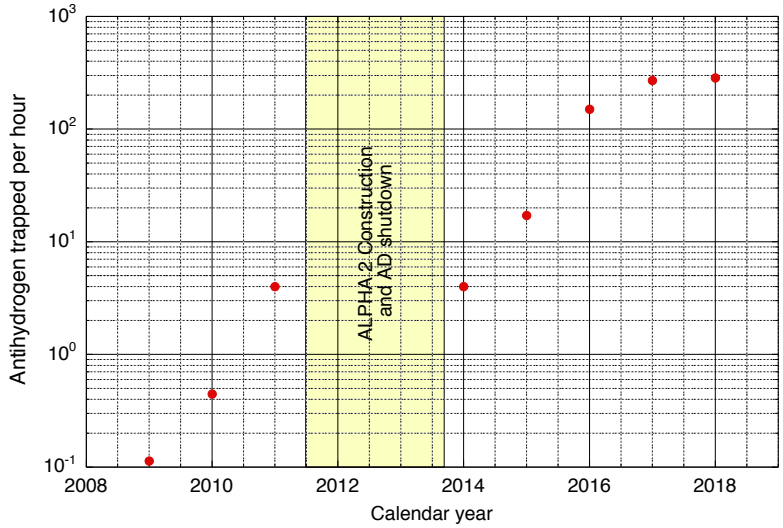

Figure 34. Historical evolution of the normalised antihydrogen trapping rate in ALPHA. The evolution (c.f. Ref. 58) has primarily, but not solely, been driven by improvements in the positron temperature.

Apart from applying our historical approach to deal with these issues, i.e. careful manipulation and control at all stages, using our full pallet of charged particle manipulation and diagnostic techniques, we are pursuing a novel strategy. The key to our strategy is based on several years of observing how, at each turn, improvements in antihydrogen trapping have been achieved primarily by reductions in the positron plasma temperature. This may seem counter-intuitive as the antiproton carries most of the momentum, but it seems consistent with simulations indicating that, in our current parameter range (as opposed to that in e.g. Madsen *et al.*[65]), antiprotons thermally equilibrate with the positrons faster than they form antihydrogen. From this observation our idea

is to use laser-cooled Be^+ ions to indirectly (sympathetically) cool the positron plasma used for antihydrogen synthesis[66]. A first demonstration of such sympathetic cooling was done by Jelenkovic et al. in 2002[67]; however, this demonstration used a ratio of 1000:1 of ions to positrons. Since Be^+ ions may potentially capture antiprotons, we have worked on a target ratio of 1:10, i.e. 100'000s of ions to cool millions of positrons.

In pursuit of this goal we implemented a Be^+ ablation source in the ALPHA-2 apparatus in 2017[68]. The source was developed to allow direct formation of ions and to allow direct (pulsed) loading of a Penning trap by ions that could propagate from the source along the magnetic field lines of our cryogenic trap. The geometry of our antihydrogen apparatus means that the closest the source can reasonably be to the trap region is at a distance of about 1.5m. The natural priority of the antihydrogen program meant that before LS2 only basic testing of the source's compatibility with the ALPHA-2 apparatus was accomplished. However, since the shutdown of the AD, we have succeeded in sympathetically cooling about 3M positrons, using about 500'000 Be+ ions, to a temperature of around 10K. This remains an unpublished first result, with both publication and much optimization to be worked out. However we are confident that this system can be brought to be operational by the end of LS2. While 10K sounds a far cry from 0.5K, our trap depth, the temperature scaling should be at least $T^{-3/2}$ [66], such that an improvement from the current start-of-the art of around 20K to 10K in itself offers an increase in trapping of at least 125%. It is expected that once the process is optimized temperatures of at least as low as 5K should be achievable [66]. Additionally, and perhaps more important, the additional cooling offered by laser-cooled Be^+ ions is likely to help combat the increased heating that is likely to ensue from the increased numbers of positrons needed to fully exploit the increased numbers of antiprotons available in the ELENA era.

In addition to their intended application of improving the antihydrogen trapping efficiency, laser-cooled Be^+ ions could also be used as a sensitive probe of the antihydrogen trapping magnetic fields in ALPHA-3 and ALPHA-g. The magnetic field dependence of the hyperfine ground-state energy levels of Be^+ ions has been measured to high levels of precision[69], and therefore measurement of the resonance frequency of the ground-state electron spin-flip transition could be used to precisely determine magnetic field strengths. Near-term antihydrogen measurements will continue to be performed with antihydrogen which is confined in a magnetic minimum trap, and the characterisation of these trapping fields will become increasingly important as we measure the properties of antihydrogen to increased levels of precision. Historically we have determined the magnetic field strength along the axis of the trap through measurements of the electron cyclotron frequency (ECR)[70]. With ongoing development, we expect that this method will be able to measure magnetic field strengths to a precision of around 1 part in 10^6 ($\sim$10 mG). It is expected that through measurements of the ground-state electron spin flip transition in Be^+, we will be able to determine the magnetic field to similar levels of precision. However another factor to consider is that the ECR method is limited to measurements of the magnetic field strength at points along the trap axis. For precision measurements of the gravitational acceleration of antihydrogen in ALPHA-g, it is likely that we will need to develop a method of measuring the magnetic field at different radial

positions within the trap. There have been recent demonstrations of optical dipole trapping of ions [71], and we are currently considering using this methodology to trap Be^+ ions. The dipole trapped ions could be moved radially throughout the trap by translating the position of the trapping laser beam, potentially allowing the magnetic field to be measured at different radial locations.

The Beryllium programme is thus currently ongoing, and requires us to be able to operate the apparatus with all the normal services (helium, cooling-water etc.) during LS2. Once we have a fully operating setup that has improved the antihydrogen trapping rate we will extend the deployment to also cover the ALPHA-g apparatus.

A new station for antihydrogen research in the ALPHA zone

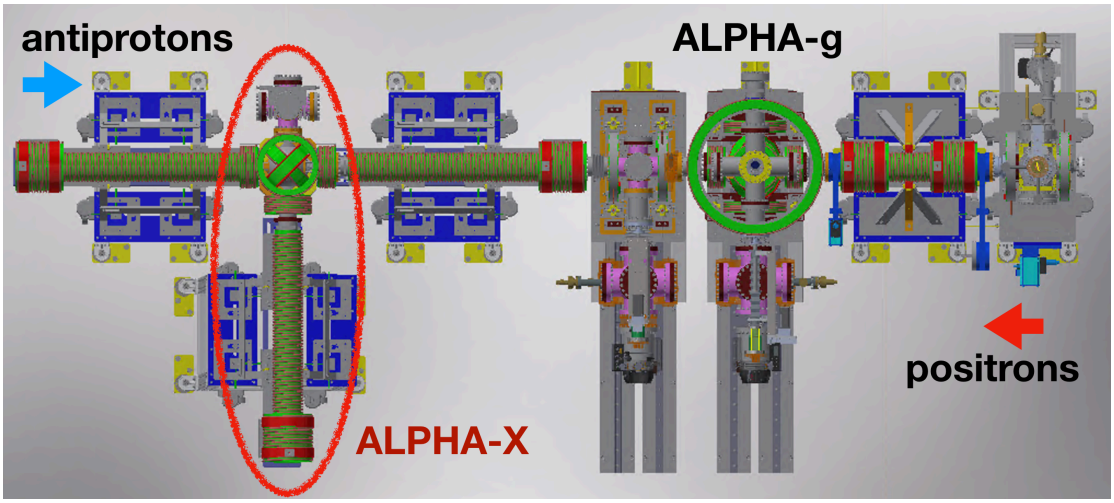

Figure 35. Diagram of ALPHA-X, the planned extension to the ALPHA-g beamline.

The main ALPHA physics program is vigorously exploiting the success of our world-leading antihydrogen trapping and spectroscopy devices. However, we anticipate ultimately reaching a limit in which the geometries and systematics of our current generation of traps hinders our ability to perform new or improved measurements. With the advent of the ELENA era, and our expanded infrastructure to support the ALPHA-g upgrade, we have included in out planning an extension to the ALPHA beamline to feed a third experimental station (ALPHA-eXtension, Figure 35) with antiprotons and positrons to develop new measurement schemes.

We are presently considering different sorts of experiments and tests to carry out at this station. With our vastly increased ability to trap antihydrogen, we can consider schemes of 'conventional' ALPHA trapping in an octupole-based trap, cooling adiabatically and through laser cooling to high phase space density, and extracting into a separate physics region. This is an underlying production principle in the antihydrogen fountain proposal described below, and could also be interesting for developing other anti-atomic interferometry experiments[72]

Importantly, this trap could be used to feed ground-state antihydrogen into beam-based experiments which could be established in magnetic-field-free regions. This could be critical for performing the highest precision measurements of gravity, hyperfine splitting, and optical transitions.

We will also be able to explore new possibilities for production of antihydrogen with high phase space density without impacting the physics progress on our operating machines. Some proposals include ideas for shrinking the size of the traps and potentially increasing optical access for carrying out experiments[73] could make future efforts more tractable.

An anti-atomic fountain

The atomic fountain is an important tool in atomic physics, allowing for long (~1 s) effective interrogation time for atomic transitions, leading to narrow transition linewidths and high precision. For example, the current standard of time is based on a Cs atomic fountain clock, reaching a precision of 10^{-16}. Also, atomic fountains form the basis for atom interferometry, a technique which provides extremely high precision measurements, for example of the gravitational interaction. Our recent demonstration of laser cooling of antihydrogen has opened the path for an entirely new class of experiments with ultra-cold antihydrogen atoms. Building upon pioneering proposals (*e.g.* [74]), we are currently developing a realistic scheme for realizing an antihydrogen fountain and anti-atomic interferometry in the ALPHA experimental zone. Our ultimate goals include a precision test of antimatter gravity via interferometry with parts per million precision, and a measurement of hyperfine splitting via Ramsey resonance with a fountain at the 10^{-9} level. If successful, these measurements will improve the precisions of the current generation of the experiments by several orders of magnitude. In addition, such a device might allow creation of antihydrogen molecular ions for a unique test of CPT involving antimatter molecules[75]. Our plan is to construct a prototype device to demonstrate proof of principle for such measurements with normal atomic hydrogen, with a goal of installing a new antihydrogen apparatus in the new ALPHA-X beamline during LS3.

Prospects for antideuterium in ALPHA

In view of the recent string of successes and our plans towards besting the current hydrogen precision on the transition in antihydrogen, it is worth taking a brief look at other longer term exotic prospects for our experiment. One exciting and exotic possibility would be to study trapped antideuterium, the bound state of an antideuteron and a positron.

Physics motivation

Like for antihydrogen, there are no theoretical predictions of any difference between deuterium and antideuterium, so the interest lies in the potential sensitivity to violation of fundamental symmetries such as Lorentz and CPT. This can be quantified through, *e.g.,* the Standard Model Extension (SME) by

Kostelecky et al.[39] . The isotope shift of the 1S-2S transition between hydrogen and deuterium is known to an absolute uncertainty of ~15 Hz[76]. The presence of the neutron in the latter opens up sensitivities to the neutron section of the so-called Standard Model Extension. Kostelecky *et al.* develop a detailed framework for deuterium though it stops short of extending the (anti)neutron argument to gravitational tests, albeit they argue that such tests could address other interesting fundamental physics. They conclude that deuterium spectroscopy is many orders of magnitude more sensitive than hydrogen spectroscopy to certain kinds of Lorentz and CPT violation, and that the same arguments hold for antideuterium and antihydrogen spectroscopy [77].

Antideuteron production and deceleration

A relatively detailed investigation of the prospect of antideuteron accumulation in the CERN AC/AA complex that predates the AD (the AD is recycled from the AC) was published by Johnson and Sherwood in 1988[78], starting from the simplest possible assumption, just assuming that antideuterons would be produced by the PS primary beam of 26 GeV/c protons on a target. The yield of antideuterons used in their discussion, based on experimental data, was 200 per 10^{13} protons on target, which should be compared to the current 30 million antiprotons for the same proton intensity, a penalty of 10^{-5}. An order of magnitude could be gained if a proton beam of 100 GeV/c was available, but the increased energy of the resulting antideuterons would of course further complicate the subsequent deceleration. Figure 38 from Ref [78] shows the relative antideuteron yield to antiproton yield as a function of proton momentum on target. Thus, assuming that this can be done as a simple extension to the current program seems a bit optimistic. If more energetic, or more intense proton or heavy ion beams could be made available, the yields would go up, as *e.g.,* proposed by Iazzi[79] or demonstrated in Au-Au collisions[80] (cf. Figure 37) but the AD complex may no longer be adapted to the resulting antideuteron beam.

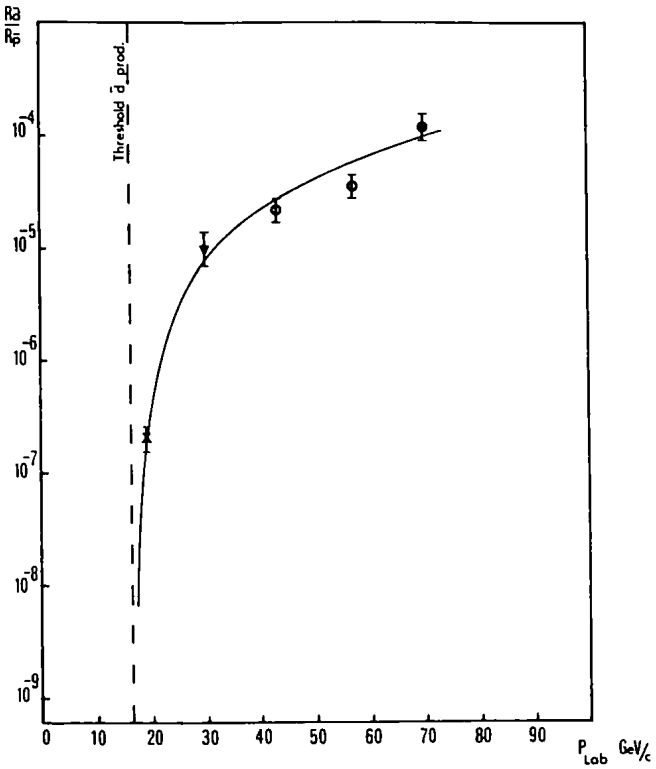

Figure 36 Experimental antideuteron/antiproton production ratios from Ref. 78.

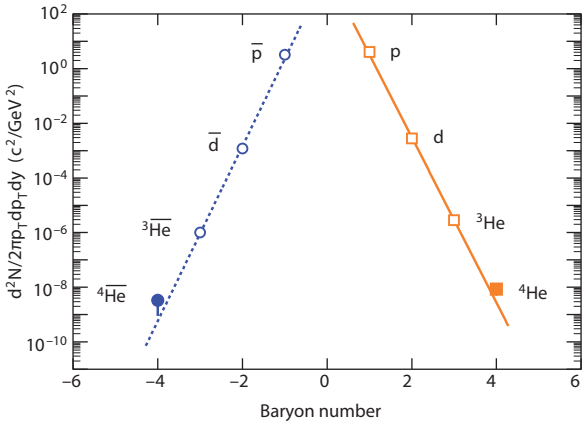

Figure 37. Differential invariant yields as a function of baryon number in Au-Au collisions; from Ref. 80.

In summary, antideuteron production and deceleration seems to be a stumbling block for studying antideuterium. However, to finish on an optimistic note, it is worth noting that the advent of ELENA has improved the prospects slightly, as the overall efficiency in bringing the antiprotons from formation to produce antihydrogen will be of order 50% with ELENA, compared to less than 1% in the past. The conversion rate from antiprotons to trapped antihydrogen in our experiment is currently around 10^{-4}, thus 200 deuterons per spill out of ELENA, would result in 1 deuterium atom in our trap every 100 mixing cycles, or

about 3 per 24h if all else remains the same. With the improvements discussed in this proposal, this number is likely to improve by at least an order of magnitude, reaching a level where physics measurements become viable (a similar yield was used in the first observation of a quantum transition in antihydrogen[3]. Thus, even quite low numbers of low energy antideuterium nuclei would make actual physics with deuterium viable.

Executive Summary

The ALPHA collaboration is proposing a multi-faceted physics program with antihydrogen in the years following LS2 and beyond. The ideas put forth here build upon our successes with trapping and studying antihydrogen atoms. We remain the only experiment with the demonstrated ability to do this. Antihydrogen physics has matured rapidly in recent years, since our first demonstration of trapping in 2010. It is no exaggeration to say that all of the physics goals imagined for antihydrogen at the inception of the AD are now within reach and likely to be exceeded. The idea of having thousands of trapped anti-atoms confined at once would have seemed absurd a decade ago; it is now routine in ALPHA.

We remain dedicated to the ambitious approach that has lead to ALPHA-2 and now to ALPHA-g. During LS2 we are both operating the ALPHA-2 machine to develop improvements to our antihydrogen capabilities and upgrading both ALPHA-g and ALPHA-2 for future physics. We wish to work with CERN and the other experiments to ensure that ELENA quickly reaches its potential and that CERN's investments and resources are efficiently utilized after LS2. We are determined to continue our 24-hour operation to fully utilize the beam from ELENA, and we hope that CERN management will work with us to provide the necessary resources to do so. We look forward to the challenges of commissioning and measuring with ALPHA-g, which will be our top priority when the beam returns after LS2. As a collaboration, we look forward to increased cooperation among AD experiments in the ELENA era, and we are open to sharing ALPHA technology with other groups if this is of interest.

We thank the SPSC for its support of our physics program over the years, and we hope that the committee will agree that the current proposal is ambitious, viable, and worthy of renewed support. Pleas address any questions to the ALPHA Spokesperson: jeffrey.hangst@cern.ch

Appendix 1: The ALPHA Collaboration

University of Aarhus, Denmark J.S. Hangst, J.T.M. McKenna, G. Stutter, S.A Jones, P. Granum
University of British Columbia, Canada T. Momose, W. Hardy. N. Evetts
University of Calgary, Canada R. Thompson, T. Friesen, A. Powell, C. So, A. Evans
University of California, Berkeley, USA J. Fajans, J. S. Wurteley, E.D. Hunter
CERN, Switzerland C.Ø. Rasmussen
Simon Fraser University, Canada M. Hayden, J. Munich
University of Liverpool, UK P. Pusa
University of Manchester, UK W. Bertsche, M. Sameed, M.A. Johnson, D. Hodgkinson, S. Fabri
Purdue University, USA F. Robicheaux
Federal University of Rio de Janeiro, Brazil C. Cesar, D.M. Silveira, R.L. Sacramento
Stockholm University, Sweden S. Jonsell
Soreq Nuclear Center, Israel E. Sarid
Swansea University, UK N. Madsen, S. Eriksson, D.P. van der Werf, M. Charlton, C.J. Baker, D. Maxwell, J.M. Jones, A. Cridland, A. Isaac, J. Peszka, P. Mullan
TRIUMF, Canada M. Fujiwara, P. Grandemange, D. Gill, A. Olin, L. Kurchaninov, K. Olchanski, A. Capra
York University, Canada S. Menary

---

[1] Andresen, G.B. *et al.* Trapped antihydrogen. *Nature* **468,** 673–676 (2010).
[2] Andresen, G. B. et al. Confinement of antihydrogen for 1000 seconds. *Nature*
[2] Andresen, G. B. et al. Confinement of antihydrogen for 1000 seconds. *Nature Physics* **7**, 558–564 (2011).
[3] Amole, C. *et al.* Resonant quantum transitions in trapped antihydrogen atoms. *Nature* **483,** 439–443 (2012).
[4] Amole, C. *et al.* Description and first application of a new technique to measure the gravitational mass of antihydrogen. *Nature Commun*. **4**, 1785 (2013).
[5] Amole, C. *et al.* Experimental limit on the charge of antihydrogen. *Nature Commun.* **5,** 3955 (2014).

[6] Ahmadi, M. *et al.* An improved limit on the charge of antihydrogen from stochastic acceleration. *Nature* **529**, 373–376 (2016).
[7] Ahmadi, M. *et al.* Antihydrogen accumulation for fundamental symmetry tests. *Nature Communications* **8**, 681 (2017).
[8] Ahmadi, M. *et al.* Observation of the 1S-2S transition in antihydrogen. *Nature* **541**, 506–510 (2017).
[9] Parthey, C.G. *et al,* Improved measurement of the hydrogen 1S-2S transition frequency. *Phys. Rev. Lett.* **107**, 203001 (2011).
[10] Ahmadi, M. et. al., Characterization of the 1S–2S transition in antihydrogen. *Nature* **557**, 71-75 (2018).
[11] Ahmadi, M. et. al., Observation of the hyperfine spectrum of antihydrogen, *Nature* **548**, 66-69 (2017).
[12] Ahmadi, M. *et. al*., Nine part-per-million measurement of the antihydrogen ground state hyperfine splitting, submitted to *Nature* (2019).
[13] Michan, J. M., Polovy, G., Madison, K. W., Fujiwara, M. C. & Momose, T. Narrowband solid state VUV coherent source for laser cooling of antihydrogen. *Hyperfine Interact.* **235**, 29–36 (2015).
[14] Ahmadi M. et. al., Observation of the 1S-2P Lyman-alpha transition in antihydrogen. *Nature* **561**, 211-215 (2018).
[15] Ahmadi, M. *et. al*., Investigation of the fine structure of antihydrogen, currently be refereed by *Nature* (2019).
[16] G. Baur *et al.*, Production of Antihydrogen, Phys. Letts. B **368**, 251 (1996)
[17] R. Neumann, Possible Experiments with Antihydrogen, in Fundamental Symmetries (Springer US), 95 (1987).
[18] H. Herr, D. Möhl and A. Winnacker, Production of and Experimentation with Antihydrogen at LEAR, in Physics at LEAR with Low-Energy Cooled Antiprotons (Springer), 659 (1984).
[19] C. G. Parthey *et al.*, Improved Measurement of the Hydrogen 1S-2S Transition Frequency, Phys. Rev. Lett. **107**, 203001 (2011).
[20] ALPHA Collaboration, In situ electromagnetic field diagnostics with an electron plasma in a Penning-Malmberg trap, New J. Phys **16**, 013037 (2014).
[21] C. Ø. Rasmussen, N. Madsen and F. Robicheaux, Aspects of 1S-2S spectroscopy of trapped antihydrogen atoms, J. Phys. B **50**, 184002 (2017).
[22] P. Wcislo, *et al.*, Experimental constraint on dark matter detection with optical atomic clocks, Nature Astro. **1**, 0009 (2016).
[23] M. S. Safronova, *et al.*, Search for new physics with atoms and molecules, Rev. Mod. Phys. **90**, 025008 (2018).
[24] C. D. Lane, Using Comparisons of Clock Frequencies and Sidereal Variation to Probe Lorentz Violation, Symmetry **9**, 245 (2017).
[25] P.H. Donnan, M.C. Fujiwara and F. Robicheaux, A proposal for laser cooling antihydrogen atoms, J. Phys. B **46**, 025302 (2013).
[26] P. Defraigne and G. Petit, CGGTTS-Version 2E: an extended standard for GNSS Time Transfer, Metrologia **52**, G1 (2015).
[27] K. Szymaniec *et al.*, NPL Cs fountain frequency standards and the quest for the ultimate accuracy, J. Phys. Conf. Ser. **723**, 012003 (2016).
[28] W. E. Lamb, Jr. and R. C. Retherford, Fine structure of the hydrogen atom by a microwave method, Phys. Rev. **72** 241 (1947).

[29] J. C. Bernauer and R. Pohl, Sci. Am. **310**, 32 (2014).
[30] R. Pohl, R. Gilman, G. A. Miller, and K. Pachucki, Annu. Rev. Nucl. Part. Sci. **63**, 175 (2013).
[31] C. E. Carlson, Prog. Part. Nucl. Phys. 82, 59 (2015).
[32] N. Bezginov, T. Valdez, M. Horbatsch, A. Marsman, A. C. Vutha, E. A. Hessels, A measurement of the atomic hydrogen Lamb shift and the proton charge radius, Science **365** 1007 (2019).
[33] R. Pohl et al., The size of the proton, Nature **466** 213 (2010).
[34] A. Antognini et al, Proton Structure from the Measurement of 2S-2P Transition Frequencies of Muonic Hydrogen, Science **339** 417 (2013).
[35] A. Beyer et al., The Rydberg constant and proton size from atomic hydrogen, Science **358** 79 (2017).
[36] H. Fleurbaey et al., New Measurement of the 1*S*−3*S* Transition Frequency of Hydrogen: Contribution to the Proton Charge Radius Puzzle, Phys. Rev. Lett. **120** 183001 (2018).
[37] N. Bezginov, T. Valdez, M. Horbatsch, A. Marsman, A. C. Vutha, E. A. Hessels, A measurementofthe atomic hydrogen Lamb shift and the protoncharge radius, Science **365** 1007 (2019).
[38] J. M. Michan, G. Polovy, K. W. Madison, M. C. Fujiwara, and T. Momose, Narrowband solid state VUV coherent source for laser cooling of antihydrogen, Hyperfine Interactions, **235**, 29 - 36 (2015).
[39] Kostelecky, V. A. & Vargas, A. J. Lorentz and CPT tests with hydrogen, antihydrogen, and related systems. Phys. Rev. D 92, 056002 (2015).
[40] Crivelli, P., Cooke, D. & Heiss, M. W. Antiproton charge radius, Phys. Rev. D 94, 052008 (2016).
[41] K.C. Harvey, Slow metastable atomic hydrogen beam by optical pumping. Journal of Applied Physics 53, 3383 (1982).
[42] S. We et al. Pulsed Sisyphus Scheme for Laser Cooling of Atomic (Anti)Hydrogen. Phys. Rev. Lett. 106, 213001 (2011).
[43] A. Bohr et al, Ionization in collisions between metastable hydrogen atoms. Phys. Rev. A 85, 042710 (2012).
[44] E. Myer, CPT tests with the antihydrogen molecular ion Phys. Rev. A 98, 010101 (2018).
[45] L. P. Yatsenko et al., Source of metastable H(2s) atoms using the Stark chirped rapid-adiabatic-passage technique. Phys. Rev. A 60, R4237(R) (1999).
[46] L. P. Yatsenko et al., Two-photon excitation of the metastable 2s state of hydrogen assisted by laser-induced chirped Stark shifts and continuum structurePhys. Rev. A 71, 033418 (2005).
[47] Blas, D., Theoretical aspects of antimatter and gravity. Philosopical Transaction of the Royal Society A 376, 20170277 (2018).
[48] Kostelecký, A. Matter-gravity couplings and Lorentz violation.Phys. Rev. D 83, 1(2011).
[49] Nieto, M. M. and Goldman, T., The arguments against “antigravity”and the gravitational acceleration of antimatter.Physics Reports 205, 5 221-228 (1991).
[50] Zhmoginov, A. Nonlinear dynamics of anti-hydrogen in magnetostatic traps: implications for gravitational measurements. Classical and Quantum Gravity30, 20 (2013).

[51] E. D. Hunter *et al.,* in preparation.
[52] Madsen, N. and Robicheaux, F and Jonsell, S. Antihydrogen trapping assisted by sympathetically cooled positrons. New Journal of Physics16, 6 063046 (2014).
[53] Capra, A. et al. JPS Conf. Proc. 18, 011015 (2017).
[54] http://garfieldpp.web.cern.ch/garfieldpp/
[55] Hamilton, P. *et al.* Antimatter Interferometry for Gravity Measurements. *Phys. Rev. Lett.* **112,** 12 (2014)
[56] S. Møller *et al.,* "Direct measurements of the stopping power for antiprotons of light and heavy targets," Phys. Rev. A, vol. 56, p. 2930, (1997).
[57] S. Møller *et al.*, "Antiproton stopping at low energies: Confirmation of velocity-proportional stopping power," Phys. Rev. Lett., vol. 88, p. 193201, (2002).
[58] Antihydrogen accumulation for fundamental symmetry tests, ALPHA Collaboration, Nature Comm. **8**, 681 (2017).
[59] Antihydrogen formation dynamics in a multipolar neutral anti-atom trap, ALPHA Collaboration, Phys. Lett. B **685**, 141 (2010).
[60] Magnetic multipole induced zero-rotation frequency bounce-resonant loss in a Penning-Malmberg trap used for antihydrogen trapping, ALPHA Collaboration, Phys. Plas. **16**, 100702 (2009).
[61] Compression of Antiproton Clouds for Antihydrogen Trapping, ALPHA Collaboration, Phys. Rev. Letts. **100**, 203401 (2008).
[62] A novel antiproton radial diagnostic based on octupole induced ballistic loss, ALPHA Collaboration, Phys. Plas. **15**, 032107 (2008).
[63] Critical loss radius in a Penning trap subject to multipole fields, J. Fajans, N. Madsen, F. Robicheaux, Phys. Plas. **15**, 032108 (2008).
[64] Antihydrogen formation, dynamics and trapping, PhD Thesis, E. Butler, (2011).
[65] Spatial Distribution of Cold Antihydrogen Formation, N. Madsen et al., Phys. Rev. Letts. **94**, 033403 (2005).
[66] Antihydrogen trapping assisted by sympathetically cooled positrons, N. Madsen, F. Robicheaux and S. Jonsell, New Jour. Phys. **16**, 063046 (2014)
[67] Sympathetically laser-cooled positrons, B.M. Jelenkovic et al., Nucl. Inst. & Meth. B **192**, 117 (2002)
[68] Ablation of Be+, M. Sameed, D. Maxwell and N. Madsen, Arxiv.
[69] Diamagnetic correction to the $^{9}Be^{+}$ ground-state hyperfine constant, N. Shiga, W. M. Itano, and J.J. Bollinger, Physical Review A **84**, 012510 (2011).
[70] *In situ electromagnetic field diagnostics with an electron plasma in a Penning-Malmberg trap*, ALPHA Collaboration, New J. Phys. **16**, 013037 (2014).
[71] *Optical trapping of an ion*, Ch. Schneider *et* al, Nature photonics, **4**, 772 (2010).
[72] Hamilton, P. *et al.* Antimatter Interferometry for Gravity Measurements. *Phys. Rev. Lett.* **112,** 12 (2014).
[73] Bertsche, W., *et al.* Cold neutral atoms via charge exchange from excited state positronium: a proposal. *New J. Phys*. **19**, 5 (2017).
[74] P.H. Hamilton et al., Antimatter Interferometry for Gravity Measurements. Phys. Rev. Lett. 112, 121102 (2014).
[75] E. Myer, CPT tests with the antihydrogen molecular ion Phys. Rev. A 98, 010101 (2018).
[76] Precision Measurement of the Hydrogen-Deuterium 1S-2S Isotope Shift, C.G. Parthey et al., Phys. Rev. Lett. **104**, 233001 (2010).

[77] Lorentz and CPT tests with clock-comparison experiments, V. A. Kostelecky and A.J. Vargas, Phys. Rev. D **98**, 036003 (2018).
[78] On the feasibility of antideuteron production and storage at CERN, C.D. Johnson and T.R. Sherwood, Hyp. Int. **44**, 65 (1988).
[79] An antideuteron beam at the JHF, F. Iazzi, Nucl. Phys A **655**, 371c (1999).
[80] Observation of the antimatter helium-4 nucleus, The STAR Collaboration, Nature **473**, 353 (2011).